Journal of Computational Physics **170,** 459–497 (2001)
doi:10.1006/jcph.2001.6745, available online at http://www.idealibrary.com on IDEAL®

Minimization of the Truncation Error by Grid Adaptation

Nail K. Yamaleev

NASA Langley Research Center, Mail Stop 128, Virginia 23681-2199
E-mail: nail@tabdemo.larc.nasa.gov

Received January 24, 2000; revised August 3, 2000

A new grid adaptation strategy, which minimizes the truncation error of a pth-order finite difference approximation, is proposed. The main idea of the method is based on the observation that the global truncation error associated with discretization on nonuniform meshes can be minimized if the interior grid points are redistributed in an optimal sequence. The method does not explicitly require the truncation error estimate, and at the same time, it allows one to increase the design order of approximation globally by one, so that the same finite difference operator reveals superconvergence properties on the optimal grid. Another very important characteristic of the method is that if the differential operator and the metric coefficients are evaluated identically by some hybrid approximation, then the single optimal grid generator can be employed in the entire computational domain independently of points where the hybrid discretization switches from one approximation to another. Generalization of the present method to multiple dimensions is presented. Numerical calculations of several one-dimensional and one two-dimensional test examples demonstrate the performance of the method and corroborate the theoretical results.

Key Words: truncation error, grid adaptation criterion, finite difference approximation, error equidistribution.

1. INTRODUCTION

Grid adaptation has now become widespread for solving multidimensional partial differential equations in arbitrary-shaped domains. One of the most important problems associated with adaptive grid generation is an essential effect of the grid point distribution on error in the numerical solution. Until the present, little attention has been paid to the fact that the concentration of grid points in regions which most influence the accuracy of the numerical solution may at the same time introduce additional error because of grid nonuniformity [1–3].

0021-9991/01 $35.00

There are two basic strategies of grid adaptation, namely, grid refinement and grid redistribution. In the first approach, grid nodes are added to locally enrich the grid to achieve higher accuracy. In the second approach, the number of grid nodes is fixed and the idea is to adjust the position of grid points to improve the numerical solution accuracy. In spite of significant distinctions, both methods require reliable and efficient grid adaptation criteria.

A number of grid adaptation criteria based on the equidistribution principle have been developed. As shown in [4] the grid point distribution is asymptotically optimal if some error measure is equally distributed over the field. One of the widely used approaches is to redistribute grid points in accordance with the arc length and the local curvature of the solution curve [5, 6]. This kind of clustering is intended to reduce the error in the vicinity of strong gradients and local extrema of the numerical solution, but it does not necessarily guarantee improvement in accuracy where the solution is smooth.

Another class of methods is based on equidistribution or minimization of the local truncation error or its estimate [7–10]. In [7] the error estimate obtained by using a finite difference approximation of the leading truncation error term is equidistributed by the grid point redistribution. Klopfer and McRae [8] solve a one-dimensional shock-tube problem with the explicit predictor-corrector scheme of MacCormack on a grid dynamically adapted to the solution. The error estimate is the leading truncation error term of the differential equations transformed to the computational coordinates. The metric coefficient is taken as a linear function of the smoothed error measure. For solving a second-order two-point boundary value problem with a centered second-order finite difference scheme, Denny and Landis [9] suggest determining the optimal coordinate mapping so that the entire truncation error vanishes at all grid points. However, this grid generator concentrates grid nodes where the solution is smooth rather than near steep gradients. Thus, the error reduction occurs in regions which do not practically affect the numerical solution accuracy. An alternative technique is employed in [10], where the optimal coordinate transformation is constructed as the solution of a constrained parameter optimization problem that minimizes a measure of the truncation error. The error measure used is a finite difference evaluation of the third derivative of the numerical solution calculated in the computational space. The main drawback of all the methods mentioned above is the fact that the error estimates do not properly take into account that part of the truncation error which is caused by the nonuniform grid spacing. Furthermore, it is not clear how to extend these methods to more general equations and discretizations, and to multiple dimensions.

A grid adaptation procedure equidistributing an error estimate of the numerical solution has been used successfully in [11] to reduce simulation error in such integral quantities as the lift or drag. This error estimate is directly related to the local residual errors of the primal and adjoint solutions of the Euler equations. The numerical results presented in [11] indicate that the order of accuracy of the integral outputs increases by one if the proposed adaptation strategy is employed. Although this approach provides significant improvement in the accuracy of the functional, the error estimation procedure is quite expensive in terms of computational time because, except for the solution of the primal problem, it is necessary to solve the adjoint Euler equations, which doubles the computational efforts.

The formulation of an adaptive mesh redistribution algorithm for boundary value problems in one dimension has been presented in [12]. The analysis uses error minimization to produce an optimal piecewise-polynomial interpolant in a given norm, which leads to the development of a family of grid adaptation criteria. Despite the fact that the present

approach works well in one dimension, this error equidistribution analysis cannot be directly extended to multiple dimensions [13].

In [14, 15] the finite element residual is applied to provide a criterion for determining where a finite element mesh requires refinement. As has been noted in [16] , for hyperbolic problems with nonsmooth solutions the finite element residual may be an ineffective error estimator, because for such problems the residual measured in the L_2 norm diverges, whereas the numerical solution converges in this norm. The problem might be overcome if the divergence of the residual is localized to the area of nonsmoothness; the residual could then be used as a local error indicator. However, the localization of discontinuities becomes a very complicated problem in multiple dimensions.

The truncation error of any differential operator obtained on a nonuniform grid can be shown to consist of two parts. The first part, which also exists on a uniform mesh, is due to the approximation of the differential operator itself. The second part is caused by the contribution to the error from the nonuniform grid spacing. As the grid is locally refined or redistributed, the first part of the error decreases, while the second part may increase considerably because of the nonuniformity of the grid. All of the equidistribution methods mentioned above redistribute grid points in accordance with one or another error estimate obtained on a nonadapted grid, but in doing so the grid adaptation itself introduces additional error, which changes the error distribution. Therefore, to account for this change in the error distribution, the grid adaptation procedure based on the error equidistribution strategy should be repeated iteratively until the error estimate norm is equally distributed over the field. Note that for moving meshes dynamically adapted to the solution, the iterative procedure should be done at each time step to attain the optimal mesh characterized by having the error equidistributed throughout the domain.

The main objective of this paper is to construct an optimal coordinate transformation so that the leading truncation error term of an arbitrary pth-order finite difference approximation is minimized so that it provides superconvergent results on the optimal grid. In contrast to the error equidistribution principle, for the present technique an *a posteriori* error estimate is not explicitly required. Furthermore, the new grid adaptation criterion allows one to minimize the error resulting from the differential operator itself and the error owing to the evaluation of the metric coefficients simultaneously. Another very attractive feature of the present approach is its applicability to hybrid approximations that depend on some basic properties of the solution, such as flow direction, sonic line, and others. If the metric coefficients are evaluated by the same hybrid discretization used for the differential operator, the new grid adaptation criterion remains valid throughout the computational domain regardless of points where the hybrid scheme switches from one approximation to another. Extension of the new adaptation criterion to multiple dimensions is presented. The numerical examples considered illustrate the ability of the method and corroborate the theoretical analysis.

2. GRID ADAPTATION IN ONE DIMENSION

The truncation error of the first derivative approximated on a 1-D nonuniform grid is considered here. Let x and ξ denote the physical and computational coordinates, respectively. Without loss of generality it is assumed that $a \le x \le b$ and $0 \le \xi \le 1$. A one-to-one

coordinate transformation between the physical and computational domains is given by

$$x = x(\xi), \tag{2.1}$$

where

$$\begin{aligned} x(0) &= a \\ x(1) &= b. \end{aligned} \tag{2.2}$$

The above mapping is assumed not singular so that the Jacobian of the transformation is a strictly positive function, i.e.,

$$x_\xi > 0, \quad \forall \xi \in [0, 1]. \tag{2.3}$$

The nonuniform grid in the physical space is obtained as images of nodes of a uniform mesh in the computational domain

$$x_i = x(\xi_i), \quad \xi_i = \frac{i}{I}, \quad i = 0, 1, \ldots, I. \tag{2.4}$$

With the coordinate transformation (2.1), the first derivative of a function $f(x)$ with respect to x can be written as follows:

$$f_x = \frac{f_\xi}{x_\xi}. \tag{2.5}$$

To construct a pth-order approximation of f_x in the physical domain, we approximate f_ξ and x_ξ by some pth-order finite difference expressions in the computational domain

$$L_h(f_x) = \frac{\sum_{l=i-l_1}^{i+l_2} \alpha_l f_l}{\sum_{m=i-m_1}^{i+m_2} \beta_m x_m}, \tag{2.6}$$

where $x_m = x(\xi_m)$, $f_l = f(\xi_l)$; L_h is a finite difference operator; and the indices l_1, l_2 and m_1, m_2, as well as the coefficients α_l and β_m, depend on particular approximations used for evaluating f_ξ and x_ξ, respectively. Henceforth, it is assumed that the functions $f(\xi)$ and $x(\xi)$ are smooth enough so that all derivatives needed for the derivation are continuous functions on $\xi \in [0, 1]$. Expanding the numerator and denominator of Eq. (2.6) in a Taylor series with respect to ξ_i and omitting the index i on the right-hand side yields

$$\begin{aligned} \sum_{l=i-l_1}^{i+l_2} \alpha_l f_l &= f_\xi + C_p^f f_\xi^{(p+1)} \Delta\xi^p + O(\Delta\xi^{p+1}) \\ \sum_{m=i-m_1}^{i+m_2} \beta_m x_m &= x_\xi + C_p^x x_\xi^{(p+1)} \Delta\xi^p + O(\Delta\xi^{p+1}), \end{aligned} \tag{2.7}$$

where

$$x_\xi^{(p+1)} = \frac{\partial^{p+1} x}{\partial \xi^{p+1}}, \quad f_\xi^{(p+1)} = \frac{\partial^{p+1} f}{\partial \xi^{p+1}}, \quad \Delta\xi = \frac{1}{I},$$

and where C_p^f and C_p^x are constants dependent on α_l and β_m, respectively. Substituting Eq. (2.7) into Eq. (2.6) and taking into account that $x_\xi > 0,\ \forall \xi \in [0, 1]$, one can write

$$L_h(f_x) = \frac{f_\xi + C_p^f \Delta\xi^p f_\xi^{(p+1)}}{x_\xi \left(1 + C_p^x \frac{\Delta\xi^p}{x_\xi} x_\xi^{(p+1)}\right)} + O(\Delta\xi^{p+1}). \tag{2.8}$$

If $\Delta\xi$ is chosen to be sufficiently small so that $\Delta\xi^p |x_\xi^{(p+1)}/x_\xi| \ll 1$, Eq. (2.8) can be linearized as follows:

$$L_h(f_x) = \frac{1}{x_\xi}\left(f_\xi + C_p^f \Delta\xi^p f_\xi^{(p+1)}\right)\left(1 - C_p^x \frac{\Delta\xi^p}{x_\xi} x_\xi^{(p+1)}\right) + O(\Delta\xi^{p+1}). \tag{2.9}$$

Note that the error introduced by the linearization is of the order of $O(\Delta\xi^{2p})$. Neglecting higher order terms in Eq. (2.9) yields

$$T_p(x) = L_h(f_x) - f_x = C_p^f \Delta\xi^p \frac{f_\xi^{(p+1)}}{x_\xi} - C_p^x \Delta\xi^p \frac{x_\xi^{(p+1)}}{x_\xi^2} f_\xi. \tag{2.10}$$

The right-hand side of Eq. (2.10) is the leading truncation error term. Thus, if the metric coefficient x_ξ is evaluated numerically as in Eq. (2.6), the asymptotic truncation error of any pth-order finite difference approximation consists of two parts: the first one resulting from the evaluation of f_ξ and the second one caused by the discretization of the metric coefficient x_ξ. It should be emphasized that any grid adaptation based on minimization or equidistribution of the first part of the truncation error alone is not sufficient because the second part of the truncation error may drastically increase in regions where $x(\xi)$ changes rapidly. In other words, any inconsistent grid adaptation transfers the error from the first term of the truncation error to the second, and vice versa. To minimize both parts of the truncation error simultaneously, the following restriction is imposed on the coordinate mapping $x(\xi)$, $\forall \xi \in [0, 1]$:

$$\left|C_p^f f_\xi^{(p+1)} x_\xi - C_p^x x_\xi^{(p+1)} f_\xi\right| \le O(\Delta\xi) x_\xi^2. \tag{2.11}$$

If Eq. (2.11) holds, the asymptotic order of approximation of Eq. (2.6) on the optimal grid generated by the mapping $x(\xi)$ is $p + 1$ in the entire computational domain. Replacing the inequality sign in Eq. (2.11) with the equality sign, the grid adaptation criterion can be expressed as

$$C_p^f f_\xi^{(p+1)} x_\xi - C_p^x x_\xi^{(p+1)} f_\xi = O(\Delta\xi) x_\xi^2. \tag{2.12}$$

Note that the presence of the $O(\Delta\xi)$ term in the above equation shows that the grid adaptation criterion is rather stable under perturbations of the optimal grid.

Recall that the coefficients C_p^f and C_p^x depend on the particular approximations used and do not depend on $f(\xi)$ and $x(\xi)$. One of the most important classes of approximation is a consistent approximation, where the same difference operator is employed to evaluate the derivatives f_ξ and x_ξ. In this case, the coefficients C_p^f and C_p^x are identical and Eq. (2.12) is simplified to

$$f_\xi^{(p+1)} - f_x x_\xi^{(p+1)} = O(\Delta\xi) x_\xi, \tag{2.13}$$

or setting the right-hand side equal to zero yields

$$f_\xi^{(p+1)} x_\xi - f_\xi x_\xi^{(p+1)} = 0. \tag{2.14}$$

There are several advantages of such a simplification. First of all, the use of the same difference approximation for both f_ξ and x_ξ eliminates the f_x term from the truncation error. Actually, let us represent f_ξ and $f_\xi^{(p+1)}$ in terms of the x derivatives:

$$\begin{aligned} f_\xi &= x_\xi f_x \\ f_\xi^{(p+1)} &= x_\xi^{(p+1)} f_x + (p+1) x_\xi^{(p)} x_\xi f_{xx} + \cdots + x_\xi^{p+1} f_x^{(p+1)}. \end{aligned} \tag{2.15}$$

With the above expressions substituted into Eq. (2.10), the leading term of the truncation error $T_p(x)$ can be written as follows:

$$T_p(x) = \left(C_p^f - C_p^x\right) \Delta\xi^p \frac{x_\xi^{(p+1)}}{x_\xi} f_x + C_p^f \Delta\xi^p \left[(p+1) x_\xi^{(p)} f_{xx} + \cdots + x_\xi^p f_x^{(p+1)}\right]. \tag{2.16}$$

Equation (2.16) shows that if $C_p^f \neq C_p^x$, then the truncation error depends on the first derivative f_x being approximated. In order to eliminate this term, the metric coefficient must be evaluated by the same difference approximation used for f_ξ. Note that if x_ξ is approximated by the exact analytical expression or any finite difference formula different from that employed to calculate f_ξ, the f_x term arises in the truncation error.

Another advantage of the consistent approximation of f_ξ and x_ξ is that the single optimal grid (in the sense of Eq. (2.14)) can be generated for hybrid discretization where the coefficient C_p^f may be discontinuous in space and implicitly may depend on the function $f(\xi)$. If $C_p^f \neq C_p^x$ and the coefficient C_p^f is discontinuous, then the optimal mapping defined by Eq. (2.12) is discontinuous as well. The identical numerical approximation of x_ξ and f_ξ removes the dependence of the optimal mapping on points in the physical domain where the hybrid scheme switches from one approximation to another. If identical numerical approximation is the case, the optimal grid point distribution depends only on the order of approximation and is completely independent of the particular finite difference formula used.

As has already been mentioned, Eq. (2.14) is a grid adaptation criterion, but at the same time this equation can be treated as a grid generation equation. To provide the existence of the solution of Eq. (2.14), it is assumed that $f_\xi > \epsilon > 0$, $\forall \xi \in [0, 1]$, and $f(\xi) \in C^{p+1}[0, 1]$. It can easily be seen that $x(\xi) = c_1 f(\xi) + c_2$ is the solution of Eq. (2.14), but this trivial solution is not appropriate because it means that $f(x)$ is a linear function of x in the physical space. Another problem associated with the solution of Eq. (2.14) is boundary conditions. Taking into account Eq. (2.15), one can show that Eq. (2.14) is a pth-order ordinary differential equation. Therefore, to find the unique solution of Eq. (2.14), p boundary conditions should be imposed, but only the two boundary conditions (2.2) are available. In spite of the above-mentioned difficulties, the optimal grid generation problem (2.14), (2.2) can be solved analytically for very important cases $p = 1, 2$, and the approximate analytical solutions can be obtained for higher order discretizations $p \geq 3$.

2.1. *First-Order Approximation,* $p = 1$

For a first-order accurate approximation p is equal to 1 in Eq. (2.13), which then takes the form

$$f_{\xi\xi} x_\xi - f_\xi x_{\xi\xi} = O(\Delta\xi) x_\xi^2. \tag{2.17}$$

By using the following expression for the second derivative,

$$f_{xx} = \frac{f_{\xi\xi} x_\xi - f_\xi x_{\xi\xi}}{x_\xi^3},$$

Eq. (2.17) written in the physical space is reduced to

$$\xi_x = \frac{f_{xx}}{O(\Delta\xi)}. \tag{2.18}$$

Integrating Eq. (2.18) and taking into account the boundary conditions $\xi(a) = 0,\ \xi(b) = 1$ yields

$$\xi(x) = \frac{\int_a^x f_{xx}\, dx}{\int_a^b f_{xx}\, dx}. \tag{2.19}$$

However, to satisfy Eq. (2.18) the following restriction should be imposed on f_{xx}:

$$\int_a^b f_{xx}\, dx = O(\Delta\xi). \tag{2.20}$$

To satisfy Eqs. (2.3) and (2.18), in this section it is assumed that $f_{xx} > 0$. As will be shown in the next section, this restriction can easily be removed. Equation (2.20) indicates that the second derivative f_{xx} has to be of the order of $O(\Delta\xi)$ for all $x \in [a, b]$. In other words, if $f(x)$ is an essentially nonlinear function, so that Eq. (2.20) is not satisfied, it is impossible to increase the global order of approximation of f_x by grid point redistribution.

In spite of the fact that the order of the approximation remains equal to 1, the global truncation error is minimized on the optimal grid Eq. (2.19). Actually, for first-order discretizations the leading truncation error term Eq. (2.10) is rewritten as

$$T_1(x) = C_1 \Delta\xi \frac{f_{\xi\xi} x_\xi - f_\xi x_{\xi\xi}}{x_\xi^2} = C_1 \Delta\xi \frac{f_{xx}}{\xi_x}, \tag{2.21}$$

where C_1 is a constant dependent on the particular first-order approximation used. The L_k norm of the truncation error, which is

$$\|T_1(x)\|_{L_k} = C_1 \Delta\xi \int_a^b \left(\frac{f_{xx}}{\xi_x} \right)^k dx, \tag{2.22}$$

can be treated as a variational integral. The corresponding Euler–Lagrange equation for minimization of the above integral is directly solvable:

$$\xi(x) = \frac{\int_a^x (f_{xx})^{k/(k+1)}\, dx}{\int_a^b (f_{xx})^{k/(k+1)}\, dx}. \tag{2.23}$$

If $k \to +\infty$, then Eq. (2.23) converts to Eq. (2.19). Therefore, the optimal mapping Eq. (2.19) minimizes the L_∞ norm of the leading truncation error term. Note that on the optimal grid Eq. (2.19), the leading truncation error term is equidistributed throughout the field, so that

$$T_1(x) = C_1 \Delta\xi \int_a^b f_{xx}\, dx = \text{const.} \tag{2.24}$$

2.2. *Second-Order Approximation,* $p = 2$

If both f_ξ and x_ξ are evaluated identically by a second-order accurate formula, the grid adaptation equation (2.13) written for $p = 2$ becomes

$$f_{\xi\xi\xi} x_\xi - f_\xi x_{\xi\xi\xi} = O(\Delta\xi) x_\xi^2. \tag{2.25}$$

The derivatives in Eq. (2.25) can be transformed from the computational space to the physical space as follows:

$$\begin{aligned} f_\xi &= f_x x_\xi \\ f_{\xi\xi\xi} &= f_{xxx} x_\xi^3 + 3 f_{xx} x_\xi x_{\xi\xi} + f_x x_{\xi\xi\xi}. \end{aligned} \tag{2.26}$$

Substituting Eq. (2.26) into Eq. (2.25) yields

$$f_{xxx} x_\xi^2 + 3 f_{xx} x_{\xi\xi} = O(\Delta\xi). \tag{2.27}$$

By using the following expressions for the metric coefficient and its derivative,

$$\begin{aligned} x_\xi &= \frac{1}{\xi_x} \\ x_{\xi\xi} &= -\frac{\xi_{xx}}{\xi_x^3}, \end{aligned}$$

and assuming that $f_{xx} \neq 0, \forall x \in [a, b]$, Eq. (2.27) can be rewritten as

$$\frac{f_{xxx}}{f_{xx}} = 3\frac{\xi_{xx}}{\xi_x} + O(\Delta\xi)\frac{\xi_x^2}{f_{xx}}. \tag{2.28}$$

Because a decrease in the last term in the above equation increases the approximation accuracy, one neglects the $O(\Delta\xi)$ term and integrates the left and right-hand sides of Eq. (2.28) with respect to x to give

$$\xi_x^3 = C f_{xx}, \tag{2.29}$$

where C is a constant of the integration. Equation (2.29) has one real and two complex roots. Since only real roots are of interest the complex roots are not considered. Taking into account the boundary conditions (2.2), the above equation can readily be integrated, which gives

$$\xi(x) = \frac{\int_a^x (f_{xx})^{1/3}\, dx}{\int_a^b (f_{xx})^{1/3}\, dx}. \tag{2.30}$$

If a grid is generated in accordance with the optimal mapping (2.30), the leading term of the truncation error is zero for all points in $[a, b]$, and the global order of accuracy is increased from 2 to 3.

The optimal grid point distribution defined by Eq. (2.30) can be applied if f_{xx} is a positive function; otherwise the mapping becomes singular, which leads to grid degeneration. However, this problem can be overcome. For that purpose the interval $[a, b]$ is divided at subintervals where f_{xx} is of constant signs. Let $x_1^- < x < x_2^-$ be an interval where the second derivative is negative: i.e., $f_{xx} = -|f_{xx}| < 0$. Then, Eq. (2.30) becomes

$$\xi(x) = \frac{\int_{x_1^-}^{x} (f_{xx})^{1/3}\,dx}{\int_{x_1^-}^{x_2^-} (f_{xx})^{1/3}\,dx} = \frac{-\int_{x_1^-}^{x} |f_{xx}|^{1/3}\,dx}{-\int_{x_1^-}^{x_2^-} |f_{xx}|^{1/3}\,dx} = \frac{\int_{x_1^-}^{x} |f_{xx}|^{1/3}\,dx}{\int_{x_1^-}^{x_2^-} |f_{xx}|^{1/3}\,dx}. \tag{2.31}$$

From Eq. (2.31) it follows that the metric coefficient ξ_x given by Eq. (2.30) is strictly positive in the interval where f_{xx} is negative. Taking into account the fact that the same formula (2.31) remains valid for positive f_{xx}, the intervals of positive and negative signs, except for the inflection points of the function $f(x)$, can be joined so that

$$\xi(x) = \frac{\sum_j \int_{x_j+0}^{x} |f_{xx}|^{1/3}\,dx}{\sum_j \int_{x_j+0}^{x_{j+1}-0} |f_{xx}|^{1/3}\,dx}, \quad \forall x : x \neq x_j, \tag{2.32}$$

where x_j are the inflection points of $f(x)$. To add the inflection points $f_{xx}(x_j) = 0$ to the above integrals, special consideration is required.

Let x_0 be a point of inflection of the function $f(x)$: i.e., $f_{xx}(x_0) = 0$. Note that if the function $f(x)$ is modified by adding an arbitrary linear function, the optimal grid (2.30) remains unchanged. Furthermore, if the function $f(x)$ is linear in the whole interval $[a, b]$, then from Eq. (2.29) it follows that $\xi_x = 0$, $\forall x \in [a, b]$. This condition results in the grid step size in the physical domain $\Delta x = \Delta\xi/\xi_x$ tending to infinity, which in turn can be interpreted that an arbitrary large grid spacing can be used to approximate the first derivative of the linear function exactly. Expanding f_{xx} in a Taylor series about $x = x_0$ in Eq. (2.30) and assuming that $f_{xxx}(x_0) \neq 0$ yields

$$f_{xx}(x) = f_{xxx}(x_0)(x - x_0) + O((x - x_0)^2).$$

Substituting the above expression in Eq. (2.30) and neglecting both $O((x - x_0)^2)$ and higher order terms gives

$$\xi_x^3 = C f_{xxx}(x_0)(x - x_0). \tag{2.33}$$

Letting $x \to x_0$ results in

$$\xi_x(x_0) = \lim_{x \to x_0} (C f_{xxx}(x_0)(x - x_0))^{1/3} = 0.$$

As noted above, this kind of grid degeneration when the metric coefficient ξ_x vanishes does not impose any restriction on the grid step size at the inflection point. Therefore, in the vicinity of the inflection point, the original second derivative f_{xx} can be modified to

$$\tilde{f}_{xx}(x) = \begin{cases} |f_{xx}|, & |f_{xx}| \geq \epsilon \\ \frac{f_{xx}^2 + \epsilon^2}{2\epsilon}, & |f_{xx}| < \epsilon \end{cases}, \tag{2.34}$$

where ϵ is a small positive parameter. Equation (2.34) provides that the metric coefficient ξ_x is a smooth function in the entire physical domain. Note that the results obtained in the foregoing section (for $p = 1$) remain valid if f_{xx} is replaced by $\tilde{f}_{xx}$.

From the above consideration, it follows that for an arbitrary $f \in C^2[a, b]$ the optimal mapping that minimizes the leading truncation error term globally is

$$\tilde{\xi}(x) = \frac{\int_a^x (\tilde{f}_{xx})^{1/3}\, dx}{\int_a^b (\tilde{f}_{xx})^{1/3}\, dx}. \tag{2.35}$$

To estimate the asymptotic truncation error of the second-order difference expression for f_x on the optimal grid (2.30), Eq. (2.8) is rewritten to include the third-order terms:

$$L_h(f_x) = \frac{f_\xi + C_2\Delta\xi^2 f_{\xi\xi\xi} + C_3\Delta\xi^3 f_\xi^{(4)}}{x_\xi + C_2\Delta\xi^2 x_{\xi\xi\xi} + C_3\Delta\xi^3 x_\xi^{(4)}} + O(\Delta\xi^4). \tag{2.36}$$

By linearizing Eq. (2.36) and collecting the terms of $O(\Delta\xi^2)$ and $O(\Delta\xi^3)$, the first two terms in the truncation error are

$$T_2(x) = C_2\frac{\Delta\xi^2}{x_\xi^2}[\, f_{\xi\xi\xi}x_\xi - x_{\xi\xi\xi}\, f_\xi] + C_3\frac{\Delta\xi^3}{x_\xi^2}\big[\, f_\xi^{(4)}x_\xi - x_\xi^{(4)}\, f_\xi\big]. \tag{2.37}$$

Because the first term on the right-hand side of Eq. (2.37) vanishes on the optimal grid defined by Eq. (2.30), the asymptotic truncation error becomes

$$T_2(x) = C_3\frac{\Delta\xi^3}{x_\xi^2}\big[\, f_\xi^{(4)}x_\xi - x_\xi^{(4)}\, f_\xi\big]. \tag{2.38}$$

To determine the expression in the square brackets, Eq. (2.14) written for $p = 2$ is differentiated with respect to ξ. Thus,

$$f_\xi^{(4)}x_\xi + f_{\xi\xi\xi}x_{\xi\xi} - f_{\xi\xi}x_{\xi\xi\xi} - x_\xi^{(4)}\, f_\xi = 0. \tag{2.39}$$

Resolving Eq. (2.14) with respect to $f_{\xi\xi\xi}$ and substituting it in Eq. (2.39) gives

$$f_\xi^{(4)}x_\xi - x_\xi^{(4)}\, f_\xi = x_{\xi\xi\xi}x_\xi^2\, f_{xx}. \tag{2.40}$$

With Eq. (2.40), the leading truncation error term on the optimal grid (2.30) can be recast as

$$T_2(x) = C_3\Delta\xi^3 x_{\xi\xi\xi}\, f_{xx}. \tag{2.41}$$

For the optimal grid, Eq. (2.30) holds. Taking that fact into account, $x_{\xi\xi\xi}$ can be represented in terms of the function $f(x)$ and its derivatives as follows:

$$x_{\xi\xi\xi} = \frac{3\xi_{xx}^2 - \xi_{xxx}\xi_x}{\xi_x^5} = \frac{5\, f_{xxx}^2 - 3\, f_x^{(4)}\, f_{xx}}{9C^3\, f_{xx}^3}, \tag{2.42}$$

where C is the integration constant in Eq. (2.29). By substituting Eq. (2.42) into Eq. (2.41) the leading truncation error term is given by

$$T_2(x) = C_3 \Delta\xi^3 \frac{5 f_{xxx}^2 - 3 f_x^{(4)} f_{xx}}{9 C^3 f_{xx}^2}. \tag{2.43}$$

This formula, which is valid for all points from the interval $[a, b]$ except for the inflection points of the function $f(x)$, shows that the error is not equidistributed on the optimal grid.

Let us estimate the leading term of the truncation error at a point of inflection x_0 : $f_{xx}(x_0) = 0$. Because the second derivative f_{xx} has been modified in the neighborhood of the inflection point, as defined by Eq. (2.34), the second-order term in the truncation error does not vanish. Substituting Eq. (2.34) into Eq. (2.37) and neglecting higher order terms gives

$$T_2(x_0) = C_2 \Delta\xi^2 \frac{-f_{xx} \tilde{f}_{xxx} (\tilde{f}_{xx})^{-2/3} + (\tilde{f}_{xx})^{1/3} f_{xxx}}{\tilde{f}_{xx}}.$$

Letting $x \to x_0$ yields

$$T_2(x_0) = C_2 \Delta\xi^2 \frac{f_{xxx}(x_0)}{(\epsilon/2)^{2/3}}. \tag{2.44}$$

Equation (2.44) shows that locally, near the inflection point, only the second order of approximation can be obtained on the optimal grid. However, if the function $f(x)$ is linear, any second-order accurate approximation of f_ξ and x_ξ in Eq. (2.5) on an arbitrary nonuniform mesh gives the exact value of f_x. By virtue of the fact that the number of inflection points is finite, the $L_k (k < K < +\infty)$ norm of the second-order accurate approximation of f_x on the optimal grid should provide superconvergent results.

In regions where the function $f(x)$ is discontinuous, the above reasoning is not valid because the first and higher derivatives do not exist there. In contrast to the inflection point, in the vicinity of local extrema of $f(x)$, where $\tilde{f}_{xx}$ achieves its maximum value, the fraction in Eq. (2.43) becomes very small, so that locally, an even higher order of accuracy may be obtained.

Remark 2.1. It can readily be checked that standard grid adaptation criteria such as the arc length of the function $f(x)$ and the second derivative f_{xx} do not globally minimize the leading term of the truncation error. Actually, with the arc length grid adaptation criterion the following grid point distribution is obtained:

$$\xi(x) = \frac{\int_a^x \sqrt{1 + f_x^2}\, dx}{\int_a^b \sqrt{1 + f_x^2}\, dx}. \tag{2.45}$$

Substituting Eq. (2.45) into Eq. (2.37) yields

$$T_2(x) = C_2 \Delta\xi^2 \frac{-3 f_x f_{xx}^2 + \left(1 + f_x^2\right) f_{xxx}}{\left(1 + f_x^2\right)^2}. \tag{2.46}$$

The comparison of Eq. (2.46) with the leading term of the truncation error obtained on a uniform grid, which is

$$T_2^{\text{un}}(x) = C_2 \Delta\xi^2 f_{xxx},$$

shows that this grid point distribution may improve the accuracy locally near steep gradients of the function $f(x)$. At the same time, in regions where f_{xx} is much greater than f_x, e.g., near local extrema of $f(x)$, the actual order of approximation may deteriorate to 1 or even less.

If instead of the arc length adaptation criterion one redistributes grid points in accordance with the second derivative f_{xx}, the leading term of the truncation error is

$$T_2(x) = -C_2 \Delta\xi^2 \frac{2 f_{xxx}}{f_{xx}^2}. \tag{2.47}$$

From the above formula it follows that in regions where $|f_{xx}| < \sqrt{2}$, the local truncation error (2.47) is always greater than the asymptotic truncation error on a uniform grid.

In summarizing what has been said above, the following conclusions can be drawn. On the one hand, the standard grid adaptation criteria do not provide superconvergence. On the other hand, although the standard grid adaptation techniques may locally improve the accuracy of calculation, the global truncation error may become even larger than that obtained on the corresponding uniform mesh. Despite the fact that the above derivation has been performed for the second-order discretization, the same conclusion can be drawn for higher order schemes.

Remark 2.2. An alternative method of solving Eq. (2.25) will now be described. Integrating Eq. (2.25) by parts and neglecting the $O(\Delta\xi)$ term on the right-hand side yields

$$f_{\xi\xi} x_\xi - f_\xi x_{\xi\xi} = \hat{C}, \tag{2.48}$$

where $\hat{C}$ is a constant of the integration. The above equation is closed by using the boundary conditions (2.2).

In order to find the unknown constant $\hat{C}$, Eq. (2.48) is rewritten in the following form:

$$x_\xi^2 \frac{\partial}{\partial\xi}\left(\frac{f_\xi}{x_\xi}\right) = \hat{C}. \tag{2.49}$$

With

$$f_{xx} = \frac{1}{x_\xi}\frac{\partial}{\partial\xi}\left(\frac{f_\xi}{x_\xi}\right),$$

Eq. (2.49) is reduced to Eq. (2.29) and the constant $\hat{C}$ can easily be determined, yielding

$$\hat{C} = \left(\int_a^b (f_{xx})^{1/3}\, dx\right)^3. \tag{2.50}$$

The boundary value problem, Eqs. (2.48), (2.50), and (2.2), should be solved numerically. If at some point f_ξ and $f_{\xi\xi}$ are equal to zero simultaneously, Eq. (2.48) degenerates. The

problem can be overcome by modifying the derivatives f_ξ, $f_{\xi\xi}$ and the constant $\hat{C}$ as

$$\tilde{f}_\xi = \frac{\tilde{f}_x}{\xi_x} = \frac{\tilde{f}_x}{(\tilde{C}\,\tilde{f}_{xx})^{1/3}}$$

$$\tilde{f}_{\xi\xi} = \frac{\tilde{f}_{xx}\xi_x - \xi_{xx}\tilde{f}_x}{\xi_x^3} = \frac{3(\tilde{f}_{xx})^2 - \tilde{f}_{xxx}\tilde{f}_x}{\tilde{C}^{2/3}(\tilde{f}_{xx})^{5/3}}$$

$$\tilde{C} = \left(\int_a^b (\tilde{f}_{xx})^{1/3}\,dx\right)^3,$$

where $\tilde{f}_{xx}$ is given by Eq. (2.34), and where $\tilde{f}_{xxx}$ and $\tilde{f}_x$ are calculated by differentiating and integrating $\tilde{f}_{xx}$ with respect to x, accordingly. Because the function $\tilde{f}_{xx}$ is strictly positive in the entire computational domain, the first derivative $\tilde{f}_\xi$ is a positive function as well. These modifications make the Eq. (2.48) fully consistent with Eq. (2.35).

Note that there are several differential forms of the optimal grid generation equation. For example, instead of integration of Eq. (2.25) by parts, Eq. (2.27) may be used to determine the optimal grid point distribution. Because each of these differential equations has its advantages and disadvantages, at the present time it is difficult to say which one is better.

2.3. *High-Order Approximations, $p \geq 3$*

If f_ξ and x_ξ are approximated identically by a third-order accurate formula, the optimal grid generation equation written in operator form in the physical space is

$$\left[\frac{1}{\xi_x}\frac{\partial}{\partial x}\right]^4 f - f_x\left[\frac{1}{\xi_x}\frac{\partial}{\partial x}\right]^4 x = 0. \tag{2.51}$$

Performing the indicated differentiation yields

$$f_{xx}\left(15\xi_{xx}^2 - 4\xi_x\xi_{xxx}\right) + \xi_x\left(-6\xi_{xx}\,f_{xxx} + \xi_x\,f_x^{(4)}\right) = 0. \tag{2.52}$$

Although the above equation is much more complicated than the analogous equation derived for the second-order discretizations, Eq. (2.28), the solution of Eq. (2.52) will be constructed in a similar form. On one hand, a solution in the form of $\xi = g(f_x)$, where g is an arbitrary function of f_x, is not appropriate because in this case the $f_x^{(4)}$ term in Eq. (2.52) cannot be canceled. On the other hand, if a solution depends on f_{xxx} or higher derivatives of $f(x)$, the $f_x^{(5)}$ term arises in the truncation error, and cannot be canceled. Therefore, the solution of Eq. (2.52) is sought in a form similar to Eq. (2.29):

$$\xi_x = C(f_{xx})^\alpha. \tag{2.53}$$

With Eq. (2.53) substituted into Eq. (2.52), the leading truncation error term can be written as

$$T_3(x) = \frac{C_3\Delta\xi^3}{(f_{xx})^{1+2\alpha}}\left[\alpha(2-11\alpha)\,f_{xxx}^2 + (4\alpha-1)\,f_{xx}\,f_x^{(4)}\right]. \tag{2.54}$$

In contrast to the second-order discretization, for the third-order approximation the leading

term of the truncation error does not vanish at any $\alpha = \text{const}$. Assuming that the parameter $\alpha(x)$ is a function that weakly depends on x and setting the leading truncation error term equal to zero yields the following quadratic equation for $\alpha(x)$:

$$\alpha(x)(2 - 11\alpha(x))\, f_{xxx}^2 + (4\alpha(x) - 1)\, f_{xx}\, f_x^{(4)} = 0. \tag{2.55}$$

The solution of Eq. (2.55) is

$$\alpha_{1,2} = \frac{1}{11}(1 + 2r(x) \pm \sqrt{1 - 7r(x) + 4r(x)^2}), \tag{2.56}$$

with

$$r(x) = \frac{f_{xx}\, f_x^{(4)}}{f_{xxx}^2}.$$

Without loss of generality it is assumed that $f_{xxx} \neq 0$. If $f_{xxx} = 0$ then the solution of Eq. (2.55) is $\alpha = 1/4$. Note that the function $\alpha(x)$ should be positive in the entire physical domain; otherwise the mapping (2.53) with $\alpha < 0$ concentrates grid points where $f(x)$ is linear and makes the grid very coarse where the second derivative f_{xx} is large. Because the above analysis is valid if the function $\alpha(x)$ depends slightly on x, α is constructed as

$$\alpha(r) = \begin{cases} \frac{1}{11}(1 + 2r + \sqrt{1 - 7r + 4r^2}), & r \leq 0 \\ -\frac{48}{343}r^3 + \frac{18}{49}r^2 - \frac{3}{22}r + \frac{2}{11}, & 0 < r < \frac{7}{4}, \\ \frac{1}{11}(1 + 2r - \sqrt{1 - 7r + 4r^2}), & r \geq \frac{7}{4} \end{cases} \tag{2.57}$$

where the polynomial in Eq. (2.57) has been chosen so that $\alpha(r)$ is a continuously differentiable function of r. A plot of α versus r is shown in Fig. 1. As can be seen in the figure,

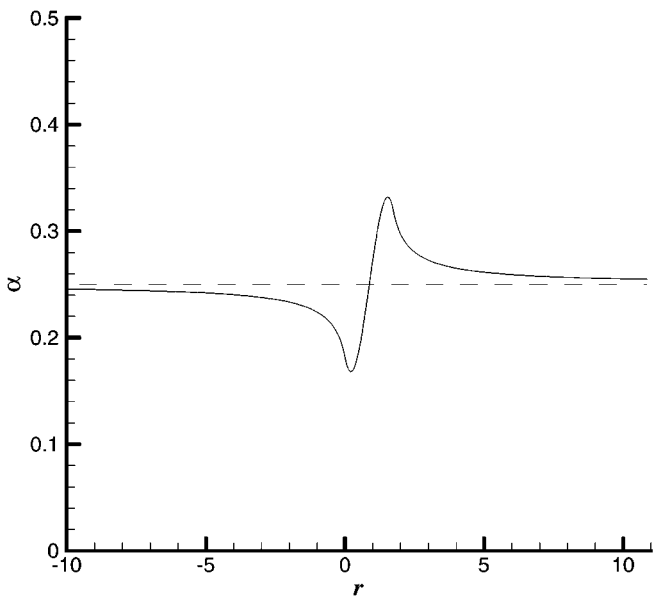

FIG. 1. Parameter α for a third-order accurate discretization.

the function $\alpha(r)$ is practically equal to $1/4$ in the whole range of r except for the interval $-1 \le r \le 3$. Although $\alpha(r)$ is quite smooth, the function $\alpha(x)$ may be nonsmooth because it depends on f_{xx}, f_{xxx}, and $f_x^{(4)}$, which are calculated numerically and may therefore be oscillatory. In numerical applications the function $\alpha(x)$ should be smoothed to meet the requirements used for the derivation of Eq. (2.54).

Such a choice of $\alpha(x)$ provides that the leading truncation error term is approximately equal to zero in the entire physical domain. As follows from Eq. (2.53), the second derivative f_{xx} must be a positive function on $[a, b]$. Note that a general property of both Eq. (2.51) and Eq. (2.14) is that if ξ_x is a solution of Eq. (2.51), then $-\xi_x$ is a solution of Eq. (2.51) as well. The same is true for the function $f(x)$ and its derivatives; i.e., if $\hat{f}_{xx} = -f_{xx}$ is substituted into Eq. (2.51), the same equation is obtained in terms of $\hat{f}_{xx}$. Hence, the second derivative f_{xx} in Eq. (2.53) can be replaced with Eq. (2.34). Thus, if f_ξ and x_ξ are evaluated by the same third-order accurate formula, the optimal grid point distribution, which minimizes the leading term of the truncation error in the entire computational domain, is

$$\xi(x) = \frac{\int_a^x (\tilde{f}_{xx})^{\alpha(x)}\, dx}{\int_a^b (\tilde{f}_{xx})^{\alpha(x)}\, dx}, \tag{2.58}$$

where $\tilde{f}_{xx}$ and $\alpha(x)$ are defined by Eq. (2.34) and Eq. (2.57), respectively.

From the above analysis one can see that the same strategy used for the third-order approximation can be applied to higher order discretizations. Actually, the leading term of the truncation error for an arbitrary pth-order approximation of f_x is

$$T_p(\xi) = \frac{C_p \Delta\xi^p}{x_\xi^2}\left(f_\xi^{(p+1)} x_\xi - f_\xi x_\xi^{(p+1)}\right). \tag{2.59}$$

With the following relations between the ξ- and x-derivatives written in operator form,

$$\frac{\partial}{\partial \xi} = \frac{1}{\xi_x}\frac{\partial}{\partial x}$$
$$\frac{\partial^n}{\partial \xi^n} = \left[\frac{1}{\xi_x}\frac{\partial}{\partial x}\right]^n,$$

the truncation error can be transformed into the physical space as follows:

$$T_p(x) = C_p \Delta\xi^p \xi_x \left(\left[\frac{1}{\xi_x}\frac{\partial}{\partial x}\right]^{p+1} f - f_x \left[\frac{1}{\xi_x}\frac{\partial}{\partial x}\right]^{p+1} x\right). \tag{2.60}$$

Expanding the power of the derivative operator yields

$$\left[\frac{1}{\xi_x}\frac{\partial}{\partial x}\right]^{p+1} f = \left[\left[\frac{1}{\xi_x}\frac{\partial}{\partial x}\right] x \left[\frac{\partial}{\partial x}\right]\right]^{p+1} f = \left[\frac{1}{\xi_x}\frac{\partial}{\partial x}\right]^{p+1} x \frac{\partial f}{\partial x} + (p+1)\left[\frac{1}{\xi_x}\frac{\partial}{\partial x}\right]^p x$$
$$\times \left[\frac{1}{\xi_x}\frac{\partial}{\partial x}\right]\frac{\partial f}{\partial x} + \cdots + \left[\frac{1}{\xi_x}\frac{\partial}{\partial x}\right] x \left[\frac{1}{\xi_x}\frac{\partial}{\partial x}\right]^p \frac{\partial f}{\partial x}. \tag{2.61}$$

Thus, the term with f_x in Eq. (2.60) is canceled, and therefore the highest derivatives of $\xi(x)$ and $f(x)$ in the truncation error $T_p(x)$ are $\xi_x^{(p)}$ and $f_x^{(p+1)}$, respectively. Assuming that on

the optimal grid the leading term of the truncation error is of the order of $O(\Delta\xi)$, $\xi(x)$ should be sought as a function of $f(x)$ and its derivatives. By comparing the highest derivatives of ξ and f, one can observe that if $\xi_x = g(f, f_x)$, then the term $f_x^{(p+1)}$ in Eq. (2.61) is never canceled, while if ξ_x is a function of $f_x^{(n)}$, $n \geq 3$ the uncancelable $f_x^{(n+p-1)}$ term arises in the truncation error $T_p(x)$. In a manner similar to the first-, second-, and third-order approximations, the optimal grid for the pth-order accurate discretization is sought in the form of Eq. (2.53). By substituting Eq. (2.53) into Eq. (2.61) the leading truncation error term becomes

$$T_p(x) = \frac{C_p \Delta\xi^p}{(f_{xx})^{p\alpha}} \left\{ [1 - \alpha(p+1)]\, f_x^{(p+1)} + \alpha G\left(\alpha, f_{xx}, f_{xxx}, \ldots, f_x^{(p)}\right) \right\}. \quad (2.62)$$

The above formula takes into account the fact that the second term on the right-hand side is proportional to α. This dependence is no surprise because for $\alpha = 0$, which corresponds to a uniform mesh, the asymptotic truncation error $T_p(x)$ is reduced to $C_p \Delta\xi^p f_x^{(p+1)}$; therefore all the terms in Eq. (2.62) except for $f_x^{(p+1)}$ have to be proportional to α. For example, for fourth- and fifth-order discretizations the leading truncation error terms obtained on the optimal grid (2.53) are

$$T_4(x) = \frac{C_4 \Delta\xi^4}{(f_{xx})^{4\alpha}} \left\{ (1 - 5\alpha)\, f_x^{(5)} + \alpha \left[-10\alpha(1 + 5\alpha) \frac{f_{xxx}^3}{f_{xx}^2} + 5(9\alpha - 1) \frac{f_x^{(3)} f_x^{(4)}}{f_{xx}} \right] \right\} \quad (2.63)$$

and

$$T_5(x) = \frac{C_5 \Delta\xi^5}{(f_{xx})^{5\alpha}} \left\{ (1 - 6\alpha)\, f_x^{(6)} + \alpha \left[(6 + 49\alpha + 196\alpha^2 + 274\alpha^3) \frac{f_{xxx}^4}{f_{xx}^3} \right.\right.$$
$$\left.\left. - (7 + 97\alpha + 421\alpha^2) \frac{f_{xxx}^2 f_x^{(4)}}{f_{xx}^2} + 3(27\alpha - 2) \frac{f_x^{(3)} f_x^{(5)}}{f_{xx}} + 2(26\alpha - 1) \frac{\left(f_x^{(4)}\right)^2}{f_{xx}} \right] \right\}, \quad (2.64)$$

respectively. As follows from Eq. (2.62), at any $\alpha = \text{const}$ the terms on the right-hand side do not vanish simultaneously. To minimize the leading term of the truncation error the following procedure is proposed. At each grid point the parameter α is found as the solution of the nonlinear equation $T(\alpha) = 0$, which is solved by Newton's method. That choice of α provides that the leading truncation error term vanishes on the optimal grid. Because the above consideration is valid only if α depends slightly on x, the function $\alpha(x)$ must be smoothed in numerical applications.

Remark 2.3. If $p \to +\infty$, i.e., if the order of approximation is infinitely large, the leading term of the truncation error (2.62) vanishes for $\alpha \to 0$. In other words, the higher the order of approximation used to evaluate f_ξ and x_ξ, the more uniform is the grid which minimizes the leading truncation error term. At the limit of infinitely high-order approximations, a uniform grid is optimal in the sense of minimization of the asymptotic truncation error.

Remark 2.4. In numerical calculations, the second derivative f_{xx} is approximated numerically and, therefore, depends on grid spacing in the physical domain. To improve the

accuracy of the optimal mapping given by Eq. (2.58), the following iteration procedure can be applied. At each grid point, the approximation of the second derivative can be updated when the new grid point distribution is found. In its turn, the updated second derivative generates a new optimal grid (Eq. (2.58)).

Let us show that this iteration technique is equivalent to the Picard iteration method (e.g., see [17]). Actually, with ξ_x replaced by $1/x_\xi$ and Eq. (2.53) integrated with respect to ξ, the following integral equation for the optimal mapping $x(\xi)$ is obtained:

$$x(\xi) = a + (b-a)\int_0^\xi G(t, x)\, dt, \tag{2.65}$$

with

$$G(t, x) = \frac{(\tilde{f}_{xx})^{-\alpha}}{\int_0^1 (\tilde{f}_{xx})^{-\alpha}\, dt}.$$

As follows from Eq. (2.34), the function G is continuously differentiable $\forall x \in [a, b]$ and, consequently, satisfies the Lipschitz condition. From this fact it follows that the integral operator Eq. (2.65) is contractive on $[a, b]$ and maps $[a, b]$ into itself. Therefore, the iteration procedure based on Eq. (2.65) converges uniformly to the optimal mapping $x(\xi)$.

An alternative way of constructing the optimal grid, when $f(x)$ is given numerically, is to interpolate $f(x)$ by using piecewise polynomials. This interpolation results in that the second derivative f_{xx} in each grid cell can be calculated analytically. Consequently, the optimal mapping Eq. (2.58) also can be calculated analytically. In contrast to the above iterative technique, no iteration is required for this approach.

3. GRID ADAPTATION IN MULTIPLE DIMENSIONS

The present approach can be extended directly to multiple dimensions. In particular, consider the three-dimensional transformation of the first derivative,

$$f_x = \frac{z_\zeta y_\eta - y_\zeta z_\eta}{J} f_\xi + \frac{y_\zeta z_\xi - z_\zeta y_\xi}{J} f_\eta + \frac{z_\eta y_\xi - y_\eta z_\xi}{J} f_\zeta, \tag{3.1}$$

where the Jacobian of the mapping is given by

$$J = x_\xi y_\eta z_\zeta + x_\eta y_\zeta z_\xi + x_\zeta y_\xi z_\eta - x_\xi y_\zeta z_\eta - x_\eta y_\xi z_\zeta - x_\zeta y_\eta z_\xi.$$

The pth-, qth-, and rth-order finite difference approximations for the ξ-, η-, and ζ-derivatives, respectively, yield

$$L_h(f_x) = \frac{(\delta_\zeta z \delta_\eta y - \delta_\zeta y \delta_\eta z)\delta_\xi f + (\delta_\zeta y \delta_\xi z - \delta_\zeta z \delta_\xi y)\delta_\eta f + (\delta_\eta z \delta_\xi y - \delta_\eta y \delta_\xi z)\delta_\zeta f}{\delta_\xi x \delta_\eta y \delta_\zeta z + \delta_\eta x \delta_\zeta y \delta_\xi z + \delta_\zeta x \delta_\xi y \delta_\eta z - \delta_\xi x \delta_\zeta y \delta_\eta z - \delta_\eta x \delta_\xi y \delta_\zeta z - \delta_\zeta x \delta_\eta y \delta_\xi z} + O(\Delta\xi^{p+1}, \Delta\eta^{q+1}, \Delta\zeta^{r+1}), \tag{3.2}$$

where the differential operators δ_ξ, δ_η, and δ_ζ are defined by

$$\begin{aligned}\delta_\xi &= \frac{\partial}{\partial\xi} + C_p\Delta\xi^p\frac{\partial^{p+1}}{\partial\xi^{p+1}}\\ \delta_\eta &= \frac{\partial}{\partial\eta} + C_q\Delta\eta^q\frac{\partial^{q+1}}{\partial\eta^{q+1}}\\ \delta_\zeta &= \frac{\partial}{\partial\zeta} + C_r\Delta\zeta^r\frac{\partial^{r+1}}{\partial\zeta^{r+1}}.\end{aligned} \tag{3.3}$$

The constants C_p, C_q, and C_r are dependent on particular pth-, qth-, and rth-order finite difference approximations applied to discretize the ξ-, η-, and ζ-derivatives accordingly. Equation (3.2) takes into account the fact that the metric coefficients are approximated by the same finite difference expressions used for evaluating f_ξ, f_η, and f_ζ.

In view of the fact that the mapping used is nonsingular ($J > 0$), the denominator of Eq. (3.2) can be linearized to give

$$\begin{aligned}T_{p,q,r}(\xi,\eta,\zeta) = \frac{1}{J}\big[&C_p\Delta\xi^p\big(\tilde F_\xi^{(p+1)} - \tilde J_\xi^{(p+1)} f_x\big) + C_q\Delta\eta^q\big(\tilde F_\eta^{(q+1)} - \tilde J_\eta^{(q+1)} f_x\big)\\ &+ C_r\Delta\zeta^r\big(\tilde F_\zeta^{(r+1)} - \tilde J_\zeta^{(r+1)} f_x\big)\big],\end{aligned} \tag{3.4}$$

where

$$\begin{aligned}\tilde F_\xi^{(p+1)} &= f_\xi^{(p+1)}(z_\zeta y_\eta - y_\zeta z_\eta) + y_\xi^{(p+1)}(z_\eta f_\zeta - z_\zeta f_\eta) + z_\xi^{(p+1)}(y_\zeta f_\eta - y_\eta f_\zeta)\\ \tilde F_\eta^{(q+1)} &= f_\eta^{(q+1)}(z_\xi y_\zeta - z_\zeta y_\xi) + y_\eta^{(q+1)}(z_\zeta f_\xi - z_\xi f_\zeta) + z_\eta^{(q+1)}(y_\xi f_\zeta - y_\zeta f_\xi)\\ \tilde F_\zeta^{(r+1)} &= f_\zeta^{(r+1)}(z_\eta y_\xi - y_\eta z_\xi) + y_\zeta^{(r+1)}(z_\xi f_\eta - z_\eta f_\xi) + z_\zeta^{(r+1)}(y_\eta f_\xi - y_\xi f_\eta)\\ \tilde J_\xi^{(p+1)} &= x_\xi^{(p+1)}(z_\zeta y_\eta - y_\zeta z_\eta) + y_\xi^{(p+1)}(z_\eta x_\zeta - z_\zeta x_\eta) + z_\xi^{(p+1)}(y_\zeta x_\eta - y_\eta x_\zeta)\\ \tilde J_\eta^{(q+1)} &= x_\eta^{(q+1)}(z_\xi y_\zeta - z_\zeta y_\xi) + y_\eta^{(q+1)}(z_\zeta x_\xi - z_\xi x_\zeta) + z_\eta^{(q+1)}(y_\xi x_\zeta - y_\zeta x_\xi)\\ \tilde J_\zeta^{(r+1)} &= x_\zeta^{(r+1)}(z_\eta y_\xi - y_\eta z_\xi) + y_\zeta^{(r+1)}(z_\xi x_\eta - z_\eta x_\xi) + z_\zeta^{(r+1)}(y_\eta x_\xi - y_\xi x_\eta).\end{aligned} \tag{3.5}$$

The linearization has been performed under the assumptions

$$\begin{aligned}\Delta\xi^p\big|\tilde J_\xi^{(p+1)}\big| &\ll J\\ \Delta\eta^q\big|\tilde J_\eta^{(q+1)}\big| &\ll J\\ \Delta\zeta^r\big|\tilde J_\zeta^{(r+1)}\big| &\ll J,\end{aligned}$$

which can be treated as conditions for the minimum number of grid points needed for the approximation.

Similar to the 1D case described above, the leading term of the truncation error (3.4) can be divided into two parts. The first part, which also exists on a uniform mesh, is due to the approximation of f_ξ, f_η, and f_ζ. The second part, which vanishes on a uniform Cartesian mesh, is caused by the evaluation of the metric coefficients. Equation (3.4) shows that if a grid is constructed so that the first term in the parentheses is of the order of $O(\Delta\xi)$, the second term is of the order of $O(\Delta\eta)$, and the third term is of the order of $O(\Delta\zeta)$ for all $\xi \in [0, 1]$, $\eta \in [0, 1]$, and $\zeta \in [0, 1]$, then the global order of approximation of the

difference operator (3.2) in ξ, η, and ζ on the optimal grid is increased from p, q, and r to $p+1$, $q+1$, and $r+1$, respectively. Therefore, in the sense of minimization of the leading truncation error term the grid adaptation criteria are

$$\tilde{F}_{\xi}^{(p+1)} - f_x \tilde{J}_{\xi}^{(p+1)} = O(\Delta\xi) J \tag{3.6}$$

$$\tilde{F}_{\eta}^{(q+1)} - f_x \tilde{J}_{\eta}^{(q+1)} = O(\Delta\eta) J \tag{3.7}$$

$$\tilde{F}_{\zeta}^{(r+1)} - f_x \tilde{J}_{\zeta}^{(r+1)} = O(\Delta\zeta) J. \tag{3.8}$$

Note that the above equations are not a system of equations and can be considered separately. If it is necessary to improve the accuracy with respect to the ξ coordinate alone, a grid must be generated such that only Eq. (3.6) holds. However, if increasing by one the order of approximation of f_x in the ξ, η, and ζ coordinates simultaneously is desirable, then the grid must obey the system of Eqs. (3.6)–(3.8).

The 3-D grid adaptation criteria (3.6)–(3.8) can be simplified. After the substitution of Eq. (3.5) into Eqs. (3.6)–(3.8) and considerable algebraic manipulation, the grid adaptation equations can be rewritten in very compact form,

$$\begin{aligned}
(z_\zeta y_\eta - y_\zeta z_\eta)\left(f_{\xi}^{(p+1)} - f_x x_{\xi}^{(p+1)} - f_y y_{\xi}^{(p+1)} - f_z z_{\xi}^{(p+1)}\right) &= O(\Delta\xi) J \\
(y_\zeta z_\xi - z_\zeta y_\xi)\left(f_{\eta}^{(q+1)} - f_x x_{\eta}^{(q+1)} - f_y y_{\eta}^{(q+1)} - f_z z_{\eta}^{(q+1)}\right) &= O(\Delta\eta) J \\
(z_\eta y_\xi - y_\eta z_\xi)\left(f_{\zeta}^{(r+1)} - f_x x_{\zeta}^{(r+1)} - f_y y_{\zeta}^{(r+1)} - f_z z_{\zeta}^{(r+1)}\right) &= O(\Delta\zeta) J,
\end{aligned} \tag{3.9}$$

where f_x, f_y, and f_z are the first derivatives with respect to the x, y, and z coordinates, respectively. One of the characteristic features of the above equations is that they do not depend on the coefficients C_p, C_q, and C_r. Consequently, if in each spatial direction the metric coefficients and the first derivatives of $f(\xi, \eta, \zeta)$ are evaluated consistently by some hybrid finite difference operators, then the grid adaptation criteria (3.9) can be applied in the whole computational domain regardless of points where the hybrid scheme switches from one approximation to another. In the 2-D case where $z_\xi = z_\eta = 0$, $z_\zeta = 1$, the 3-D grid adaptation criteria (3.9) are reduced to

$$\begin{aligned}
y_\eta\left[f_{\xi}^{(p+1)} - f_y y_{\xi}^{(p+1)} - f_x x_{\xi}^{(p+1)}\right] &= O(\Delta\xi) J \\
-y_\xi\left[f_{\eta}^{(q+1)} - f_y y_{\eta}^{(q+1)} - f_x x_{\eta}^{(q+1)}\right] &= O(\Delta\eta) J.
\end{aligned} \tag{3.10}$$

If, in addition to these conditions, $y_\xi = y_\zeta = 0$, $y_\eta = 1$ are imposed, Eqs. (3.9) are reduced to the 1-D optimal grid generation equation (Eq. 2.13). Similar to Eq. (2.13), Eqs. (3.9) and (3.10) can be proved to be invariant with respect to stretching and to translation of both the physical and computational coordinates. Note especially that because all the grid adaptation criteria, Eqs. (2.13), (3.9), and (3.10), have been obtained in the L_∞ norm, these criteria remain valid in any L_k norm.

As follows from the analysis presented in the foregoing section, the grid adaptation equation does not ensure that the coordinate mapping obtained as the solution of Eq. (2.14) is not singular. The singular mapping means that either $J \le 0$ or $J \to +\infty$. Because Eq. (3.9) is converted to Eq. (3.10) and in its turn Eq. (3.10) is reduced to Eq. (2.14) if the dimension of the space is decreased by 1, the same singularity may occur in two and three dimensions as well.

Equations (3.9) and (3.10) must be closed by corresponding boundary conditions. Similar to the 1-D case, these equations can be shown to be pth-order partial differential equations. Therefore, for each equation in Eq. (3.9), p boundary conditions should be imposed at each pair of the opposite boundaries (i.e., $\xi = 0$ and $\xi = 1$, $\eta = 0$ and $\eta = 1$, $\zeta = 0$ and $\zeta = 1$) to find the unique solution. However, at each boundary only one boundary condition is available. For example, in the 3-D case in the ξ coordinate, the boundary conditions are

$$\xi(x, y, z) = 0, \quad \xi(x, y, z) = 1. \tag{3.11}$$

In other words Eq. (3.9) and Eq. (3.10) are not closed. The situation becomes even more uncertain when only one of the grid adaptation criteria is used. However, this uncertainty gives additional degrees of freedom, and at the same time it is conceivable that there exists more than one optimal grid that satisfies the criteria (3.9) or (3.10). From this standpoint, both Eq. (3.10) and Eq. (3.9) should be treated as the grid adaptation criteria rather than the optimal grid generation equations.

One of the most general structured grid generation strategies is based on the variational approach proposed by Brackbill and Saltzmann [18]. In this method a grid is generated as the solution of the minimization problem. By forming the variational principle with a linear combination of the integral measures of smoothness, orthogonality, and adaptation, a system of elliptic equations is derived. The new grid adaptation criteria can be incorporated into this approach by constructing an integral measure of adaptation so that the Euler–Lagrange equations associated with the minimization of this integral alone give Eq. (3.9). On one hand, the minimax principle guarantees that the coordinate mapping obtained as the solution of this minimization problem is not singular [19]. On the other hand, the new grid adaptation criteria provide that the leading term of the truncation error is minimized so that the finite difference approximation Eq. (3.2) calculated on the optimal grid exhibits superconvergence properties.

Remark 3.1. In spite of the fact that the present analysis has been performed for the first derivative f_x, it can be directly extended to an equation or a system of equations, which can be represented as

$$f_x(u) = g(x), \tag{3.12}$$

where $g(x)$ is a given function. For example, the steady-state 1-D Burgers equation written in conservation law form is

$$\frac{\partial}{\partial x}\left(\frac{u^2}{2} - \mu\frac{\partial u}{\partial x}\right) = 0, \tag{3.13}$$

where μ is a positive constant. A comparison of Eq. (3.13) and f_x shows that for the Burgers equation the optimal grid can be constructed by using Eq. (2.58) with

$$f(x) = \frac{u^2}{2} - \mu\frac{\partial u}{\partial x}. \tag{3.14}$$

It should be pointed out that the above conclusion is valid if the second derivative $u_{xx} = (u_x)_x$ and the convective term $(u^2/2)_x$ are approximated consistently.

In real numerical applications, the exact analytical solution is unknown. The problem can be overcome by using the numerical solution, which approximates the exact solution,

to build the monitor function $f(x)$. As mentioned earlier, because of the presence of the $O(\Delta\xi)$ term on the right-hand side of Eq. (2.13), the optimal grid is rather stable to perturbations caused by numerical approximation of Eq. (2.58). The same conclusion is drawn for the multidimensional grid adaptation criteria. Therefore, one can say with reasonable confidence that the optimal grid generated by using the numerical solution should preserve its superconvergence property. An analogous technique is applied to unsteady problems. To generate the optimal grid at each time step, the unknown monitor function can be constructed by using the numerical solution taken from the previous time step.

The same approach can be applied to the Euler and Navier–Stokes equations. The 1-D Euler and Navier–Stokes equations can be written in conservation law form as

$$\frac{\partial \mathbf{F}}{\partial x} = 0, \tag{3.15}$$

where for the Euler equations $\mathbf{F}$ is the inviscid flux $\mathbf{F}_{\text{in}}$ and for the Navier–Stokes equations $\mathbf{F}$ is the inviscid flux minus the viscous flux $\mathbf{F}_{\text{in}} - \mathbf{F}_{\text{vis}}$.

As follows from Eq. (3.9), any component of the vector $\mathbf{F}$ can be chosen as a function with respect to which a grid is adapted. Although that choice provides increase in accuracy for this particular vector component, it may not result in decrease in the truncation error for the remaining vector components. In fact, as many components as the vector $\mathbf{F}$ has, that many optimal grids can be generated. Since the different vector components may have strong gradients and local extrema in different regions of the physical domain, this kind of grid adaptation is not effective. In such a case the monitor function $f(x)$ can be obtained by using the method of least squares. Because the optimal grid generation equations are invariant with respect to stretching of the function $f(x)$ and its derivatives, the second derivatives of F^n, $n = \overline{1, N}$ can be normalized as

$$\tilde{F}^n_{xx}(x) = \frac{\left|F^n_{xx}\right|}{\max\limits_x \left|F^n_{xx}\right|}. \tag{3.16}$$

The result is that all of the vector components are of the same order and, consequently, make proportional contributions to the second derivative f_{xx} used to generate the optimal grid (Eq. (2.58)). The resulting function f_{xx} is obtained as the solution of the minimization problem,

$$\sum_{i=0}^{I} \sum_{n=1}^{N} \left[\tilde{F}^n_{xx}(x_i) - f_{xx}(x_i)\right]^2 \to \min \tag{3.17}$$

in the least squares sense. The function f_{xx} constructed in this fashion allows one to generate a grid which is optimal for the whole vector $\mathbf{F}$ rather than for its particular component. Note that the power in Eq. (3.17) should be chosen in accordance with the power of the L_k norm in which the solution of the Euler or Navier–Stokes equations is sought.

4. RESULTS AND DISCUSSION

To validate the applicability and efficiency of the new method, several 1-D and one 2-D test examples are considered. For each 1-D test function, five series of calculations have

been executed on different grids with the same number of grid points. The first calculation is done on a uniform grid; the second uses the standard grid adaptation criterion based on the arc length or the second derivative of the test function; the third is performed on the optimal grid obtained as the analytical solution of Eq. (2.14); the fourth employs the optimal grid (2.58) generated numerically by using the following approximation for the second derivative:

$$(f_{xx})_i = \frac{h_i f_{i+1} - (h_i + h_{i+1}) f_i + h_{i+1} f_{i-1}}{h_i h_{i+1}(h_i + h_{i+1})/2}, \quad h_i = x_i - x_{i-1}. \tag{4.1}$$

This formula is reduced to the second-order three-point central approximation of f_{xx} if an equispaced grid in the physical domain is used. The integrals in Eq. (2.58) are computed with trapezoidal rule integration. As a result of this integration, the strictly increasing function $\xi(x)$ is obtained and is then reversed by using a third-order accurate piecewise spline interpolation. The fifth calculation is also executed on the uniform grid; however, instead of a pth-order approximation, a $(p+1)$th-order accurate discretization is applied to calculate both f_ξ and x_ξ. At each boundary, one-sided pth-order differences are used for f_ξ and x_ξ.

To estimate the accuracy of the method, the pth-order finite difference approximation of f_x is compared with the exact value of the first derivative calculated at the same grid node in the L_2 norm. The order of approximation is estimated on successively refined grids, the coarsest of which contains 20 cells and the finest 2560 cells.

4.1. *1-D Test Examples*

Second-order approximation, $p = 2$. The first test example is an evaluation of the first derivative of $f(x) = x^m$, $0 \le x \le 1$ by using a second-order central difference for f_ξ and x_ξ. When m is sufficiently large, this function has a boundary layer of width $O(1/m)$ near $x = 1$. For this test case, the exact optimal grid point distribution defined by Eq. (2.25) can be found analytically:

$$x_{\text{opt}}(\xi) = \xi^{\frac{3}{m+1}}. \tag{4.2}$$

In contrast to [9] the new grid adaptation criterion provides the concentration of grid nodes near the boundary layer of the function $f(x)$.

An error convergence plot for this test function ($m = 23$) is presented in Fig. 2. As one might expect, the L_2 norm of the truncation error calculated on a uniform grid exhibits the $O(\Delta\xi^2)$ convergence rate that is consistent with the second order of accuracy of the central differences. However, the same second-order approximation of f_x on the optimal grid (4.2) exhibits the convergence rate which is higher than $O(\Delta\xi^3)$. Although the accuracy of f_x obtained on the adaptive grid (2.30) with f_{xx} evaluated by Eq. (4.1) is slightly less compared to results of the optimal grid (4.2), the order of approximation is about 3.5. To show the superiority of the present method over the standard grid adaptation criterion (2.45), the truncation error that is calculated on grids adapted in accordance with the arc length of $f(x)$ is also shown in Fig. 2. In spite of the fact that the standard grid adaptation technique slightly improves the accuracy of calculation in comparison with the equispaced grid point distribution, the convergence rate is less than $O(\Delta\xi^2)$. The fact should be emphasized that the new grid adaptation criterion (2.30) not only provides superconvergent results, but as

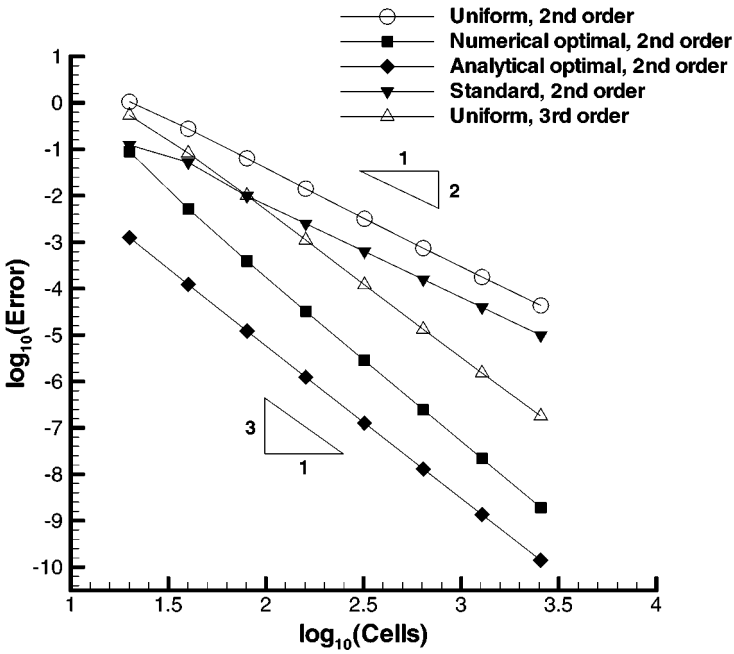

FIG. 2. Error convergence for a second-order approximation of f_x of $f(x) = x^m$, calculated on (1) uniform grid, (2) optimal grid generated numerically, (3) analytical optimal grid, (4) grid adapted in accordance with the arc length criterion, and (5) uniform grid with third-order accurate discretization.

compared with the uniform grid results on the finest mesh, reduces the error by six orders of magnitude.

An advantage of the consistent grid adaptation (2.14), which is based on the fact that the truncation errors resulting from the approximations of f_ξ and x_ξ cancel each other, becomes obvious when the optimal grid results are compared with those obtained by using a third-order accurate approximation on a uniform grid. Figure 2 shows that both the second-order approximation on the optimal grid and the third-order discretization on the uniform grid with the same number of grid points have the $O(\Delta\xi^3)$ convergence rate. However, the optimal grid results are about 10^3 times more accurate.

Note that the optimal grid (Eq. (4.2)) is essentially nonsmooth and does not meet the standard criterion of smoothness, which is $|x_{\xi\xi}/x_\xi| < O(1)$ [19]. Furthermore, the optimal mapping (4.2) is singular at the point $\xi = 0$ where $x_\xi \to \infty$. In spite of this fact, the above comparisons corroborate the theoretical analysis and demonstrate the advantage of the new grid adaptation criterion over the standard approaches.

Another very useful characteristic feature of the new method is its generality, in the sense that, if a single second-order hybrid discretization is used for both f_ξ and x_ξ, the same optimal mapping (4.2) minimizes the leading truncation error term. To demonstrate this property, the error convergence of the hybrid approximation obtained on the uniform and optimal grids with the same number of grid points are depicted in Fig. 3. The hybrid difference operator is constructed as follows:

$$\left(\frac{\partial f}{\partial \xi}\right)_i = \begin{cases} \frac{1}{2\Delta\xi}(f_{i+1} - f_{i-1}), & i \text{ even} \\ \frac{1}{2\Delta\xi}(-3f_i + 4f_{i+1} - f_{i+2}), & i \text{ odd.} \end{cases} \tag{4.3}$$

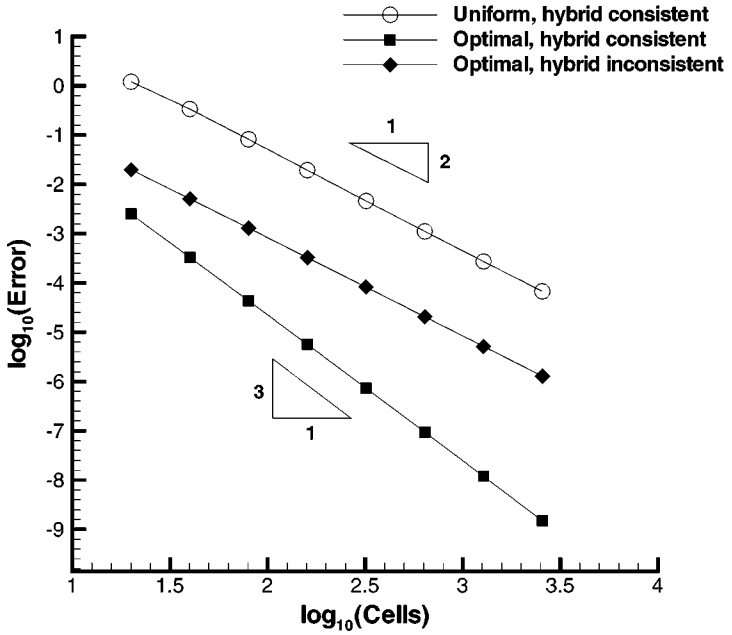

FIG. 3. Error convergence of a second-order hybrid approximation of f_x of $f(x) = x^m$, calculated with the consistent and inconsistent discretizations of the metric coefficient on the optimal and uniform grids.

The identical approximation is employed for the metric coefficient x_ξ. A comparison shows that the global order of the consistent approximation of f_ξ and x_ξ is increased by 1 on the same optimal grid (4.2) used for the nonhybrid approximation. As has been shown in Section 2, the approximation of the metric coefficient and the first derivative f_ξ should be the same; otherwise the optimal mapping defined by Eq. (2.30) does not minimize the leading truncation error term. To show that the discretization of the metric coefficient plays a crucial role in reduction of the truncation error, a two-point central difference expression is used to approximate x_ξ in the whole computational domain, while the same hybrid scheme (4.3) is used for f_ξ. An error convergence plot for this inconsistent approximation, which is also depicted in Fig. 3, shows that if the metric coefficient is evaluated in a different way than f_ξ, the order of approximation on the optimal grid deteriorates to 2. Also, Fig. 3 shows that the truncation error increases by a factor of 10^3 in comparison with the consistent discretization results.

The second test function considered is

$$f(x) = \frac{1}{(e^m - 1)x + 1}, \quad 0 \le x \le 1. \tag{4.4}$$

In the present test example, the parameter m was chosen to be 5. This function has a boundary layer of width $O(m/(e^m - 1))$ at $x = 0$. For this function the optimal grid generation equation (Eq. 2.14), which depends on the order of approximation rather than on a particular type of discretization, can be solved analytically, yielding

$$x_{\text{opt}}(\xi) = \frac{e^{m\xi} - 1}{e^m - 1}. \tag{4.5}$$

It should be emphasized that Eq. (2.30) yields the same optimal mapping as Eq. (4.5).

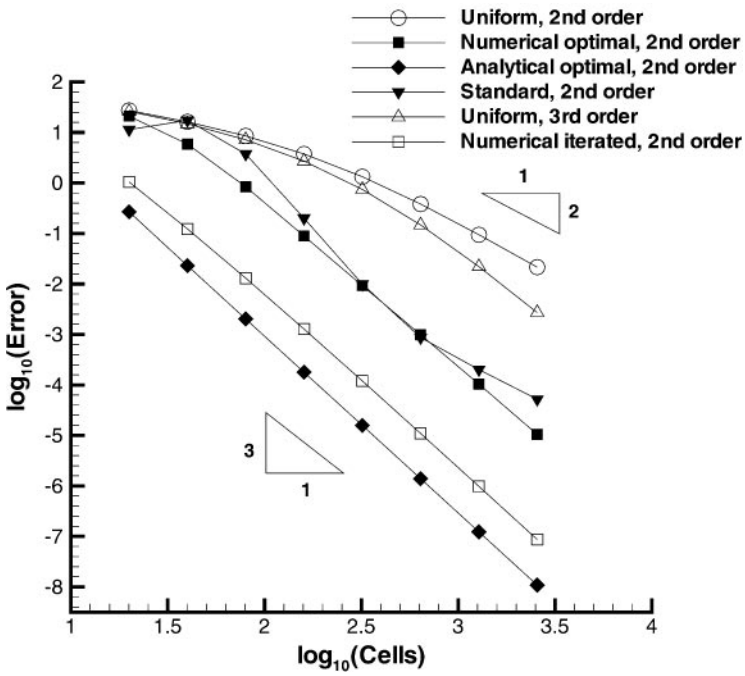

FIG. 4. Error convergence for a second-order approximation of f_x of Eq. (4.4), calculated on (1) uniform grid, (2) optimal grid generated numerically, (3) analytical optimal grid, (4) grid adapted in accordance with the arc length criterion, (5) uniform grid with third-order accurate discretization, and (6) numerical optimal grid generated iteratively.

The optimal grid (4.5) is the well-known exponential coordinate transformation, which is widely used in the literature (e.g., [1, 9]) for solving boundary layer problems. However, the mapping (4.5) is optimal only for a special class of functions, such as Eq. (4.4), and not optimal for other functions. Similar to Figs. 2 and 3, error convergence plots for the second-order symmetric and hybrid discretizations (4.3) are depicted in Figs. 4 and 5, respectively. These figures show that the error obtained on the optimal grid has a convergence rate of $O(\Delta\xi^{3.5})$ that is even higher than follows from the theoretical analysis. The optimal grid point distribution constructed by the numerical integration of Eq. (2.30) reduces the truncation error by about four orders of magnitude compared to the uniform grid results, but does not provide the same accuracy as the optimal grid (4.5). The accuracy can be improved if the iteration procedure described in Remark 2.4 is applied. For this test problem, 15 to 20 iterations were needed to reach convergence. No attempt was made to optimize the iteration process. Referring to Fig. 4 one can see that this procedure considerably increases the accuracy and provides practically the same convergence rate as the analytical optimal grid (4.5).

The importance of the metric coefficient evaluation is illustrated in Fig. 5. Analogous to the foregoing test case, the inconsistent discretization of f_ξ and x_ξ leads to decreases in both the order and accuracy of the approximation. When the metric coefficient and the first derivative f_ξ are evaluated by using the same hybrid operator (4.3), the convergence rate obtained on the optimal grid (4.5) becomes $O(\Delta\xi^3)$.

From the present theoretical analysis it follows that the new grid adaptation strategy may be quite sensitive to the inflection points of the function $f(x)$. In order to verify this

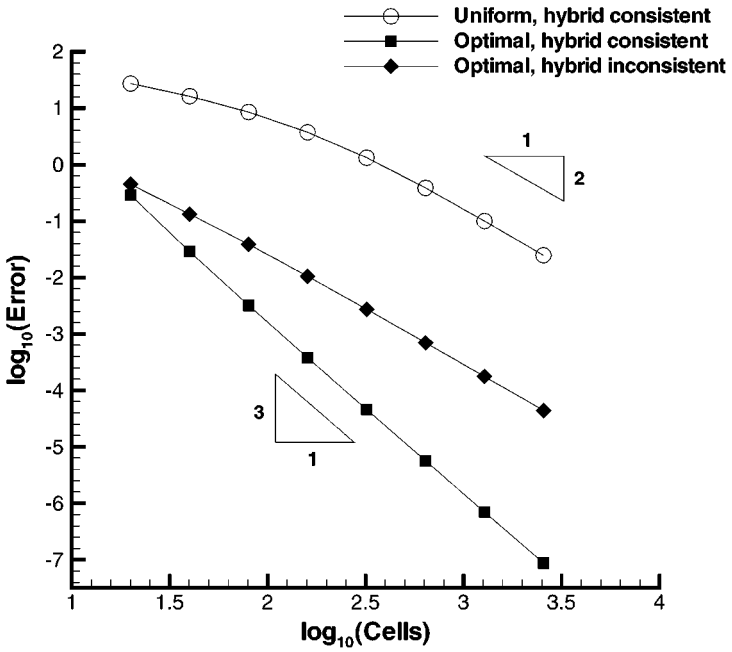

FIG. 5. Error convergence of a second-order hybrid approximation of f_x of Eq. (4.4), calculated with the consistent and inconsistent discretizations of the metric coefficient on the optimal and uniform grids.

conclusion, the following function,

$$f(x) = \frac{1}{36m^2}\left[\sin(3mx) - 27\sin(mx)\right], \quad 0 \le x \le \pi, \tag{4.6}$$

which has m inflection points, has been chosen as a test function. Despite the presence of the inflection points where $f_{xx} = 0$, it is possible to construct the optimal mapping analytically without using Eq. (2.34). It can be done if the optimal grid (2.30) is generated in each interval of constant signs of f_{xx} separately:

$$x_{\text{opt}}(\xi) = \frac{\pi}{m}(j-1) + \frac{1}{m}\arccos\left[2j - 2m\xi - 1\right], \quad \frac{j-1}{m} \le \xi \le \frac{j}{m}, \quad j = \overline{1, m}. \tag{4.7}$$

In numerical calculations the parameter m was taken to be 5. The above optimal coordinate transformation obeys Eq. (2.30) in the entire physical domain except at the inflection points.

Figures 6 and 7 are analogous to Figs. 2 and 3, accordingly. As one can see in Fig. 6, the presence of the inflection points results in the convergence rate being $O(\Delta\xi^{2.5})$, which is lower than predicted by the theoretical analysis. Nevertheless, the optimal grid adaptation reduces the truncation error by a factor of 20 in comparison with the uniform grid results. One of the reasons for such a behavior is that high-order derivatives of the function $f(x)$ in Eq. (4.6) are well bounded, which makes the approximation of f_x on the uniform grid sufficiently accurate. The use of the standard grid adaptation criterion based on $\tilde{f}_{xx}$ (Eq. (2.34)) leads to deterioration of the convergence rate to $O(\Delta\xi^{1.5})$, and at the same time the L_2 norm of the truncation error is about 50 times less accurate than the uniform grid results. Figure 7 shows that the inconsistent approximation of f_ξ and x_ξ increases the

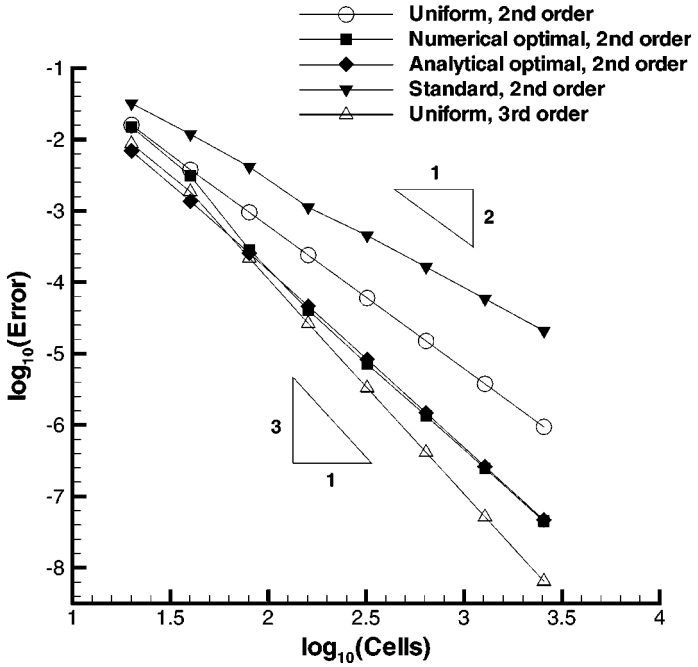

FIG. 6. Error convergence for a second-order approximation of f_x of Eq. (4.6), calculated on (1) uniform grid, (2) optimal grid generated numerically, (3) analytical optimal grid, (4) grid adapted in accordance with the $\tilde{f}_{xx}$ criterion, and (5) uniform grid with third-order accurate discretization.

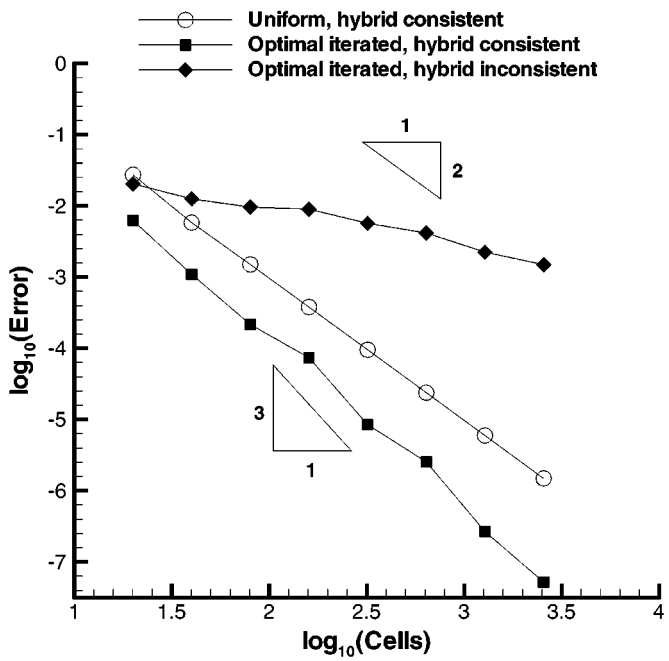

FIG. 7. Error convergence of a second-order hybrid approximation of f_x of Eq. (4.6), calculated with the consistent and inconsistent discretizations of the metric coefficient on the optimal and uniform grids.

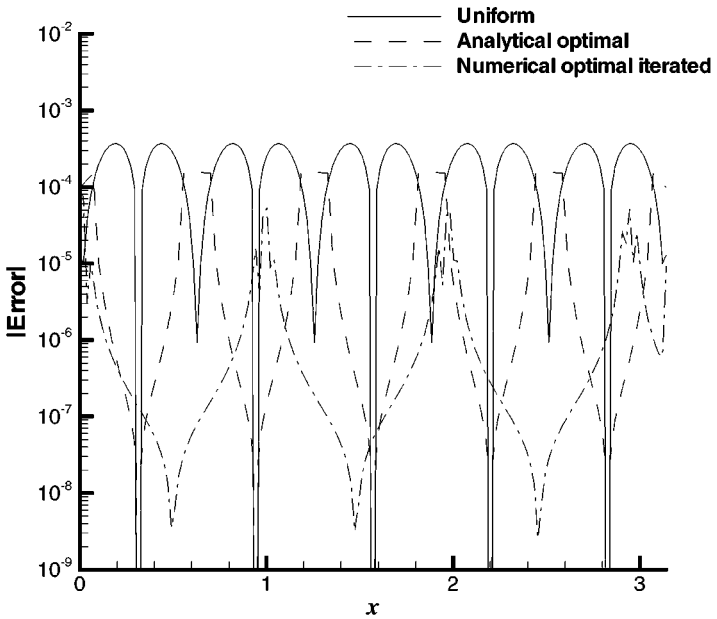

FIG. 8. Pointwise error distribution for a second-order approximation of f_x of Eq. (4.6), calculated on the analytical optimal, numerical optimal, and corresponding uniform grids.

truncation error by five orders of magnitude in comparison with the consistent approximation results calculated on the optimal grid.

To give greater insight into where the maximum error occurs, pointwise error distributions obtained on both the uniform and optimal grids are shown in Fig. 8. As expected, the truncation error calculated on the optimal grid achieves its maximum values at the inflection points, while the maximum error on the uniform grid occurs at points where the third derivative $|f_{xxx}|$ is large. In contrast to the uniform grid, the most accurate approximation of the first derivative f_x on the optimal grid is near the local extrema of $f(x)$. Using Eq. (2.34) instead of f_{xx} results in a gain in accuracy in the vicinity of the inflection points. Figure 8 presents a pointwise error plot obtained by this method as well. The error distribution obtained on the optimal grid is essentially nonuniform, which gives an indication of the difference between the present and equidistribution grid adaptation criteria.

From the practical point of view, it is very important to improve the accuracy of calculation when the function $f(x)$ has an interior layer. In this test example, the function

$$f(x) = \frac{2\epsilon x\left[17 + 73(\epsilon x)^2 + 55(\epsilon x)^4 + 15(\epsilon x)^6\right]}{15\pi[1 + (\epsilon x)^2]^4} + \frac{2}{\pi}\arctan(\epsilon x), \quad -1 \le x \le 1 \quad (4.8)$$

is considered. In the calculations, the parameter ϵ was taken to be 10^3, which results in the function (4.8) having a pronounced interior layer of width $O(1/\epsilon)$ at $x = 0$. This function has been chosen so that the optimal grid point distribution (2.30) can be integrated analytically. As in the foregoing example, the singularity ($x_\xi \to +\infty$) in the optimal mapping (2.30), resulting from the inflection point at $x = 0$, can be overcome by generating the optimal grid

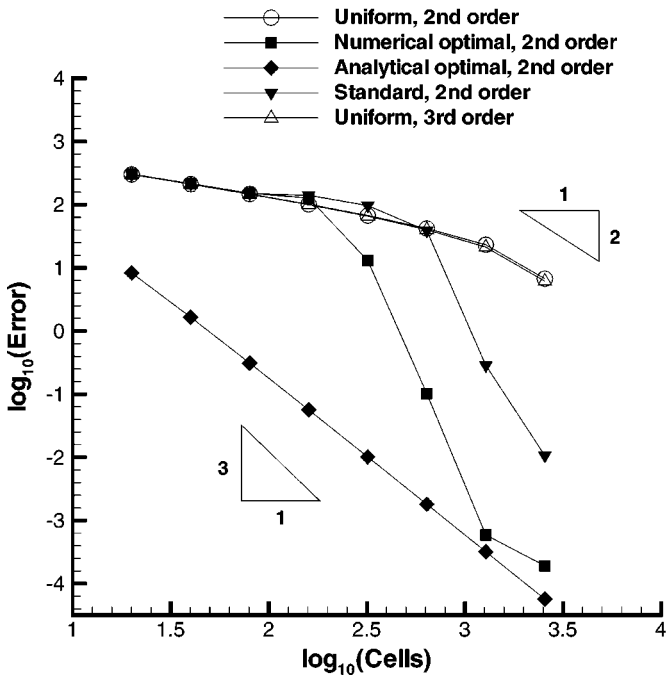

FIG. 9. Error convergence for a second-order approximation of f_x of Eq. (4.8), calculated on (1) uniform grid, (2) optimal grid generated numerically, (3) analytical optimal grid, (4) grid adapted in accordance with the arc length criterion, and (5) uniform grid with third-order accurate discretization.

in the $-0.5 \le x < 0$ and $0 \le x \le 0.5$ intervals separately, which gives

$$x_{\text{opt}}(\xi) = \begin{cases} -\sqrt{\frac{1-2\xi}{1+2\epsilon^2\xi}}, & 0 \le \xi < 0.5 \\ \sqrt{\frac{2\xi-1}{1+2\epsilon^2(1-\xi)}}, & 0.5 \le \xi \le 1. \end{cases} \tag{4.9}$$

In Fig. 9 the error convergence of the symmetric second-order discretization of f_x evaluated on the optimal grid (4.9) is compared with results obtained by second- and third-order approximations on a uniform grid. Figure 9 also shows the truncation error calculated on grids generated by using the standard (2.45) and new (2.30), (2.34) grid adaptation criteria. Because the internal layer thickness is comparable with the finest grid spacing, none of the uniform grids considered can provide second-order results. For the analytical optimal grid, the convergence rate is of the order of $O(\Delta\xi^{2.5})$. Although it is less than the theoretical limit, the truncation error on the finest mesh (2560 cells) has been reduced by more than five orders of magnitude compared to the uniform grid results. The standard grid adaptation criterion (Eq. (2.45)), which is widely used to improve the resolution of steep gradients of the solution, does not provide the cancellation of the leading truncation error term. Therefore, these results are about two orders of magnitude less accurate than those obtained on the optimal grid (2.30), (4.1), (2.34), as is evident in Fig. 9.

A comparison of the hybrid approximation (4.3) on different grids and with different approximations for the metric coefficient x_ξ is presented in Fig. 10. If f_ξ and x_ξ are evaluated identically, the same optimal grid (4.9) provides superconvergent results, while if these approximations are different, the convergence rate is even less than $O(\Delta\xi^2)$.

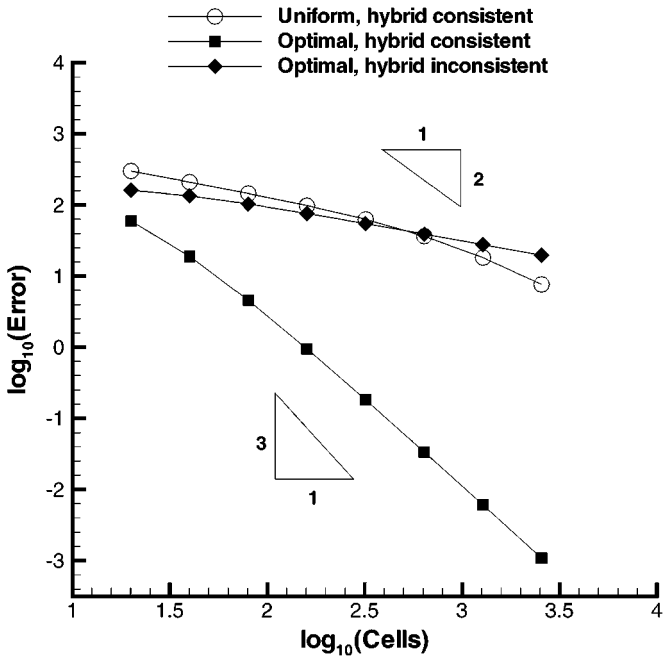

FIG. 10. Error convergence of a second-order hybrid approximation of f_x of Eq. (4.8), calculated with the consistent and inconsistent discretizations of the metric coefficient on the optimal and uniform grids.

High-order approximations, $p \geq 3$. For a third-order discretization the optimal grid generation equation, (2.55), cannot be solved analytically; however, the solution can be found in the approximate form of Eqs. (2.57) and (2.58). The same function (4.4), used in the second example, is taken as a test function. The first derivative f_ξ and the metric coefficient are evaluated by a third-order accurate formula as

$$(g_\xi)_i = \frac{1}{6\Delta\xi}\left(-2g_{i-1} - 3g_i + 6g_{i+1} - g_{i+2}\right), \tag{4.10}$$

where $g(\xi)$ is either $f(\xi)$ or $x(\xi)$.

Figure 11 shows error convergence plots obtained on the optimal (2.57), (2.58), and uniform grids with the same number of grid cells. Although for the mapping (2.57), (2.58), the leading term of the truncation error is approximately equal to zero, the error convergence rate obtained on the optimal grid is about $O(\Delta\xi^{3.8})$, which corroborates the theoretical results. Note that the same iterative technique used earlier for the second-order approximations can be applied in the present case as well. However, because of the fact that the optimal coordinate transformation (2.57), (2.58) is the approximate solution of Eq. (2.55), the iterations do not practically improve the accuracy of calculation. Therefore, the results are not presented here.

The truncation error can be reduced if the optimal grid generation equation (2.52) is solved numerically. To avoid the solution of the third-order differential equation, a new dependent variable, $u(x) = \xi_x$, is introduced. Then Eq. (2.52), which is a second-order differential equation in terms of $u(x)$, is integrated numerically on a uniform grid constructed in the physical domain. To close Eq. (2.52), the metric coefficient ξ_x is taken to be proportional to $(\tilde{f}_{xx})^{1/4}$ at the boundaries. The metric coefficient ξ_x found in this way is integrated, and

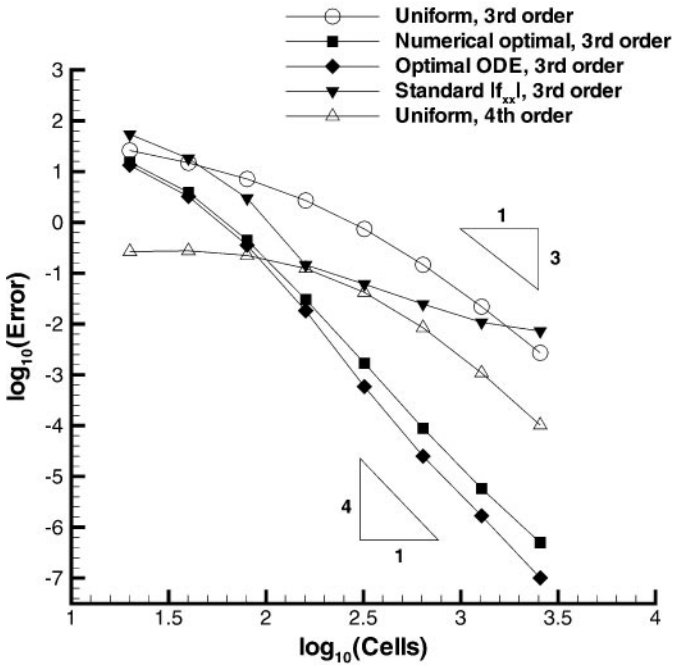

FIG. 11. Error convergence for a third-order approximation of f_x of Eq. (4.4), calculated on (1) uniform grid, (2) optimal grid generated numerically, (3) analytical optimal grid, (4) grid adapted in accordance with the $\tilde{f}_{xx}$ criterion, and (5) uniform grid with fourth-order accurate discretization.

the optimal grid point distribution is obtained by a third-order accurate piecewise spline interpolation of the function $\xi(x)$. As one can see in Fig. 11, these optimal grid results exhibit a convergence rate of essentially $O(\Delta\xi^4)$ and provide higher accuracy than results calculated on the optimal grid (2.57), (2.58).

To demonstrate the superiority of the optimal grid adaptation over the equispaced grid point distribution, an error convergence plot of a symmetric fourth-order accurate approximation of f_x, calculated on a uniform grid with the same number of grid points, is also depicted in Fig. 11. The L_2 norm of the truncation error of the third-order approximation (4.10) on the optimal grid is reduced by a factor of several hundred in comparison with the fourth-order accurate results obtained on the uniform grid.

Error convergence plots for the following hybrid approximation,

$$\left(\frac{\partial f}{\partial \xi}\right)_i = \begin{cases} \frac{1}{6\Delta\xi}\left(-2f_{i-1} - 3f_i + 6f_{i+1} - f_{i+2}\right), & i \text{ even} \\ \frac{1}{6\Delta\xi}\left(-11f_i + 18f_{i+1} - 9f_{i+2} + 2f_{i+3}\right), & i \text{ odd} \end{cases}, \tag{4.11}$$

calculated on the optimal and corresponding uniform grids, are shown in Fig. 12. The optimal grid results are about four to five orders of magnitude more accurate than those obtained on the finest uniform grid. However, if the metric coefficient is evaluated by Eq. (4.10) in the entire computational domain while the approximation of f_ξ remains the same Eq. (4.11), the error convergence rate of this inconsistent discretization becomes even less than $O(\Delta\xi^3)$ as the grid is refined.

The next test example is a fourth-order accurate approximation of the first derivative of the function $f(x) = x^m$, where the parameter m has been chosen to be 49. The first

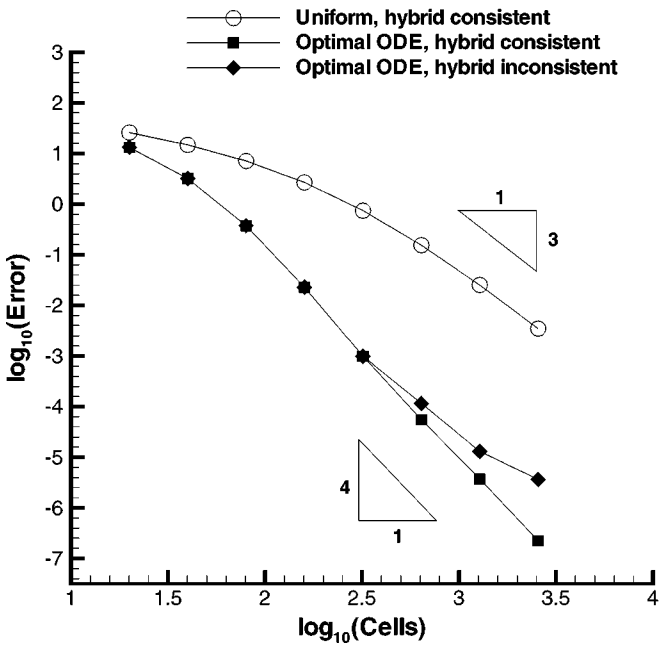

FIG. 12. Error convergence of a third-order hybrid approximation of f_x of Eq. (4.4), calculated with the consistent and inconsistent discretizations of the metric coefficient on the optimal and uniform grids.

derivatives f_ξ and x_ξ are discretized by a five-point symmetric approximation,

$$(g_\xi)_i = \frac{1}{12\Delta\xi}\left(g_{i-2} - 8g_{i-1} + 8g_{i+1} - g_{i+2}\right), \tag{4.12}$$

where $g(\xi)$ is either $f(\xi)$ or $x(\xi)$. If the order of approximation p is an even number, then for $f(x) = x^m$ the optimal grid generation of Eq. (2.14) can be solved analytically:

$$x_{\text{opt}}(\xi) = \xi^{\frac{p+1}{m+1}}. \tag{4.13}$$

The above mapping is optimal in the sense of the minimization of the leading truncation error term if $m > p$; otherwise any pth-order accurate difference expression approximates the first derivative f_x exactly. If the parameter m is fixed to be sufficiently large, one can observe that as the order of approximation p is increased, the optimal grid (4.13) becomes more uniform; this characteristic correlates with the above theoretical analysis. The optimal grid point distribution can also be calculated numerically by using Eq. (2.58). At each grid point the unknown parameter $\alpha(x)$ is found as a solution of the equation

$$T_4(\alpha) = 0, \tag{4.14}$$

where $T_4(\alpha)$ is given by Eq. (2.63). For this particular choice of the function $f(x)$, Eq. (4.14) can be solved analytically:

$$\alpha = \frac{1}{5}\frac{m-4}{m-2}. \tag{4.15}$$

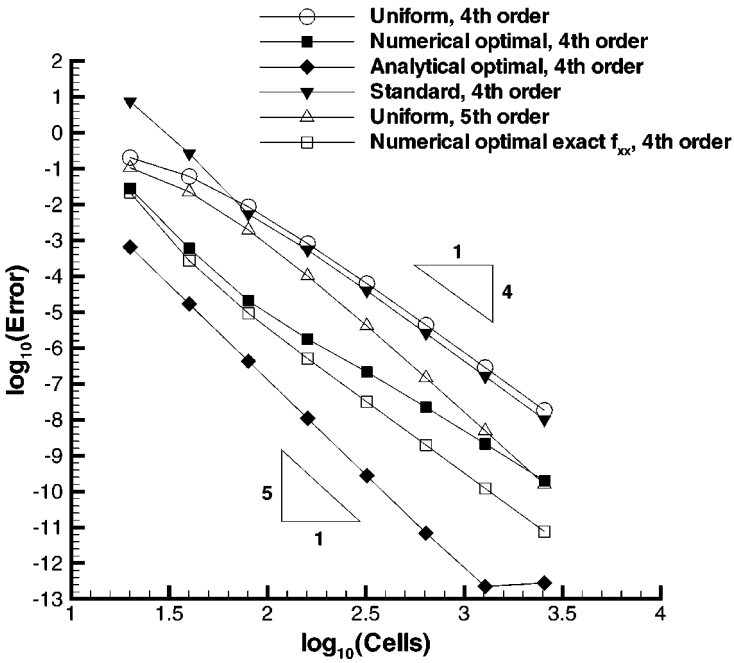

FIG. 13. Error convergence for a fourth-order approximation of f_x of $f(x) = x^m$, calculated on (1) uniform grid, (2) optimal grid generated numerically, (3) analytical optimal grid, (4) grid adapted in accordance with the arc length criterion, (5) uniform grid with fifth-order accurate discretization, and (6) numerical optimal grid generated with the exact f_{xx}.

Note that the optimal mapping (2.58), (4.15) is identical to the mapping (4.13) if $p = 4$. Error convergence plots calculated on the analytical (4.13) and numerical (2.58), (4.15) optimal grids as well as on the corresponding uniform grid are shown in Fig. 13. As one can see in this figure, the fourth-order approximation (4.12) on the optimal grid (4.13) exhibits an even higher convergence rate than $O(\Delta\xi^5)$, which allows one to reduce the L_2 norm of the truncation error by six orders of magnitude in comparison with the uniform grid results. The optimal grid (2.58), (4.15), generated numerically, provides superconvergent results only on coarse grids, while as the grid is refined the order of approximation deteriorates to 4. This deterioration results from the numerical approximation of both the second derivative and the integral in Eq. (2.58). Nevertheless, the evaluation of f_x on the 80-cell optimal grid (2.58), (4.15) is about three orders of magnitude more accurate than that on the uniform grid with the same number of grid points. One of the main reasons for such a behavior is an error introduced by the numerical approximation of f_{xx} in Eq. (2.58). As mentioned above, the optimal mapping (4.13) is singular $x_\xi \to +\infty$ at $\xi = 0$, which considerably decreases the accuracy of the f_{xx} approximation (4.1). This perturbation introduced into the optimal grid by the numerical evaluation (4.1) destroys the superconvergence property. However, if one uses the exact expression for f_{xx} despite the fact that the integral in Eq. (2.58) and $x(\xi)$ are calculated numerically, the order of approximation is practically recovered to its optimal value (see Fig. 13).

To demonstrate the importance of the consistent approximation of f_ξ and x_ξ, error convergence plots calculated by using different hybrid approximations on the optimal and corresponding uniform grids are depicted in Fig. 14. The fourth-order accurate hybrid

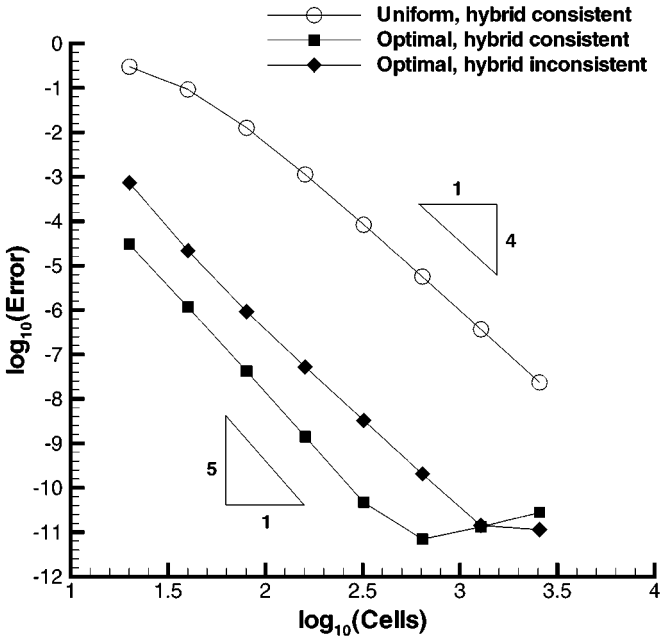

FIG. 14. Error convergence of the fourth-order hybrid approximation of f_x of $f(x) = x^m$, calculated with the consistent and inconsistent discretizations of the metric coefficient on the optimal and uniform grids.

approximation is constructed as follows:

$$(f_\xi)_i = \begin{cases} \frac{1}{12\Delta\xi}\,(f_{i-2} - 8f_{i-1} + 8f_{i+1} - f_{i+2}), & i \text{ even} \\ \frac{1}{12\Delta\xi}\,(-3f_{i-1} - 10f_i + 18f_{i+1} - 6f_{i+2} + f_{i+3}), & i \text{ odd.} \end{cases} \tag{4.16}$$

If the metric coefficient x_ξ is evaluated by the same difference expression employed for the first derivative f_ξ (4.16), then the leading term of the truncation error vanishes on the optimal grid (4.13). Figure 14 shows the truncation error of the consistent hybrid approximation of f_ξ and x_ξ exhibits a convergence rate of $O(\Delta\xi^5)$. At the same time, if the metric coefficient is discretized by the symmetric fourth-order accurate formula (4.12) in the entire computational domain, while the same approximation (4.16) is used for f_ξ, the convergence rate deteriorates to $O(\Delta\xi^4)$ and the truncation error increases by a factor of 50–100 in comparison with the consistent approximation results. The deterioration of the error convergence rate on the finest optimal mesh presumably is caused by the machine accuracy.

4.2. *2D Test Example*

We shall seek a particular solution of Eq. (3.10) in the form

$$\begin{aligned} f(\xi,\eta) &= \mathrm{e}^{\alpha\xi}\mathrm{e}^{\beta\eta} \\ x_{\mathrm{opt}}(\xi,\eta) &= \mathrm{e}^{\gamma\xi}\mathrm{e}^{\phi\eta} \\ y_{\mathrm{opt}}(\xi,\eta) &= \mathrm{e}^{\theta\xi}\mathrm{e}^{\psi\eta}, \end{aligned} \tag{4.17}$$

where α, β, and γ, ϕ, θ, ψ are given and unknown constants, respectively. Note that this choice of f, x, and y uniquely defines the function $f(x, y)$ in the physical domain. Because the above mapping must be nonsingular, the Jacobian of the mapping,

$$J(\xi, \eta) = (\gamma\psi - \phi\theta)\mathrm{e}^{(\gamma+\theta)\xi}\mathrm{e}^{(\phi+\psi)\eta}, \tag{4.18}$$

should be positive in the whole computational domain, which leads to

$$\gamma\psi - \phi\theta > 0. \tag{4.19}$$

Substituting Eq. (4.17) into the first equation of (3.10) yields

$$(\gamma\psi - \phi\theta)\alpha^3 = (-\phi\alpha + \gamma\beta)\theta^3 + (\psi\alpha - \theta\beta)\gamma^3. \tag{4.20}$$

Equation (4.20) together with the constraint (4.19) gives a family of the optimal grids. Assuming that $\phi = \psi = \beta = 1$ simplifies the equation considerably. Under this assumption Eqs. (4.20) and (4.19) are reduced to

$$(\gamma - \theta)\alpha^3 = (\gamma - \alpha)\theta^3 + (\alpha - \theta)\gamma^3 \tag{4.21}$$

and

$$\gamma - \theta > 0, \tag{4.22}$$

respectively. Equation (4.21) has three real roots

$$\begin{aligned} \gamma_1 &= \alpha - \theta, \\ \gamma_2 &= \theta, \\ \gamma_3 &= \alpha. \end{aligned} \tag{4.23}$$

The roots γ_2 and γ_3 are not appropriate because the second root does not meet the inequality (4.22), while the third root implies that $f(x) = x$. Therefore, the only nontrivial solution of Eqs. (4.21) and (4.22) is $\gamma + \theta = \alpha$. By introducing a parameter m so that $\gamma/\theta = m$, the particular solution of Eq. (3.10) can be written in the following form:

$$\begin{aligned} x_{\mathrm{opt}}(\xi, \eta) &= \mathrm{e}^{\frac{-m\alpha}{m+1}\xi}\mathrm{e}^{\eta} \\ y_{\mathrm{opt}}(\xi, \eta) &= \mathrm{e}^{\frac{-\alpha}{m+1}\xi}\mathrm{e}^{\eta} \\ f(x, y) &= x^{-\frac{m+2}{m-1}} y^{\frac{2m+1}{m-1}}. \end{aligned} \tag{4.24}$$

In the present test example the parameters m and α have been chosen to be 10 and 3, respectively. The corresponding optimal 41×21 grid and 30 isolines of the function $f(x, y)$ are depicted in Fig. 15. Notably, the optimal grid is orthogonal neither in the domain nor at the boundaries. Moreover, the grid lines are concentrated near strong gradients, and at the same time, they are not strictly aligned to the isolines of $f(x, y)$. A second-order accurate approximation of f_x is obtained by using two-point central differences for all the ξ and η derivatives. A uniform grid is generated by the transfinite interpolation of the boundary nodes, which are uniformly distributed along the boundaries. Because the optimal grid

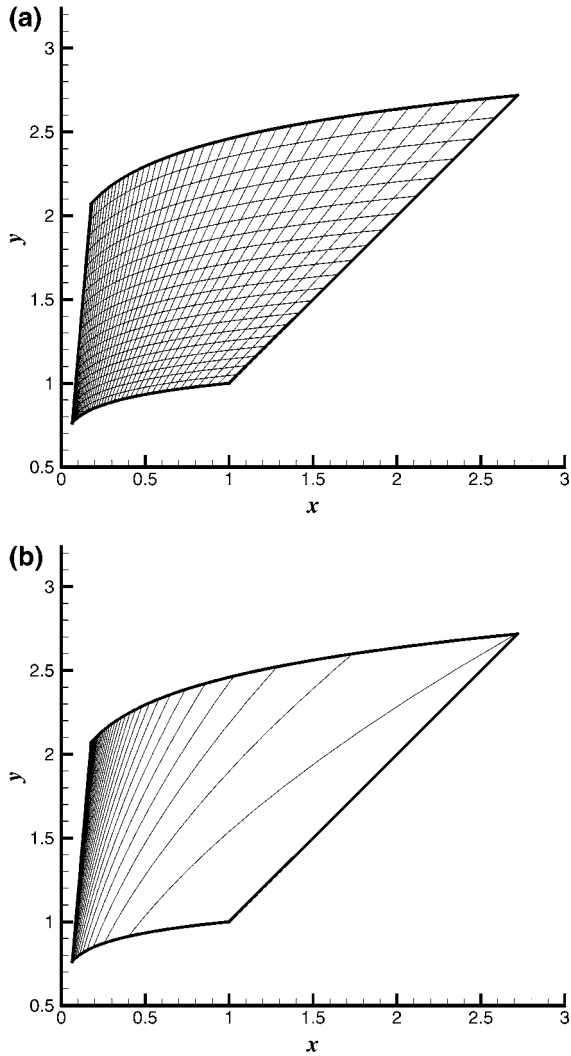

FIG. 15. Optimal 40×20 grid and 30 isolines of the function $f(x)$, Eq. (4.24).

(4.24) has been constructed under the assumption that the leading term of the truncation error in the ξ coordinate vanishes on the optimal grid, the grid is refined only in ξ, while the number of grid cells in η is fixed and equal to 20. Note that the grid refinement in the η coordinate does not influence the convergence rate of the truncation error, which is consistent with Eq. (3.10).

A comparison of the truncation error convergences obtained on the optimal and uniform grids is shown in Fig. 16. Similar to the 1-D test examples, the global order of the symmetric second-order approximation in two dimensions is increased by more than 1 on the optimal grid. Furthermore, the L_2 norm of the truncation error on the finest mesh is about four orders of magnitude less than that obtained on the corresponding uniform grid. As can be seen in Fig. 16, the new grid adaptation criterion enables one to reach the asymptotic convergence rate on coarse grids, while the application of a third-order accurate discretization on the uniform grid does not result in such essential reduction in the truncation error as on the optimal grid.

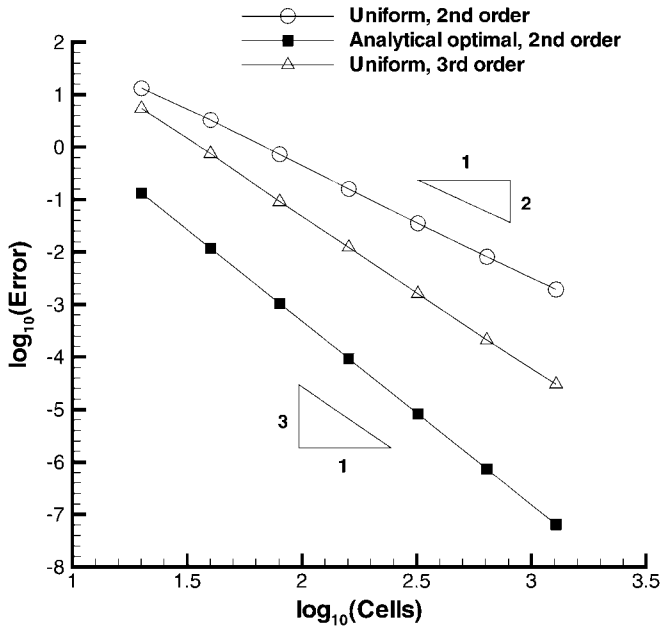

FIG. 16. Error convergence for a second-order approximation of f_x of Eq. (4.24), calculated on (1) uniform grid, (2) analytical optimal grid, and (3) uniform grid with third-order accurate discretization.

The importance of the identical approximations of the first derivatives f_ξ and f_η and the metric coefficients x_ξ, y_ξ, and x_η, y_η, respectively, is illustrated in Fig. 17. The figure shows that if f_ξ, x_ξ, and y_ξ are evaluated by the same hybrid discretization (4.3), the order of approximation in ξ is increased by 1 if grid points are redistributed in accordance

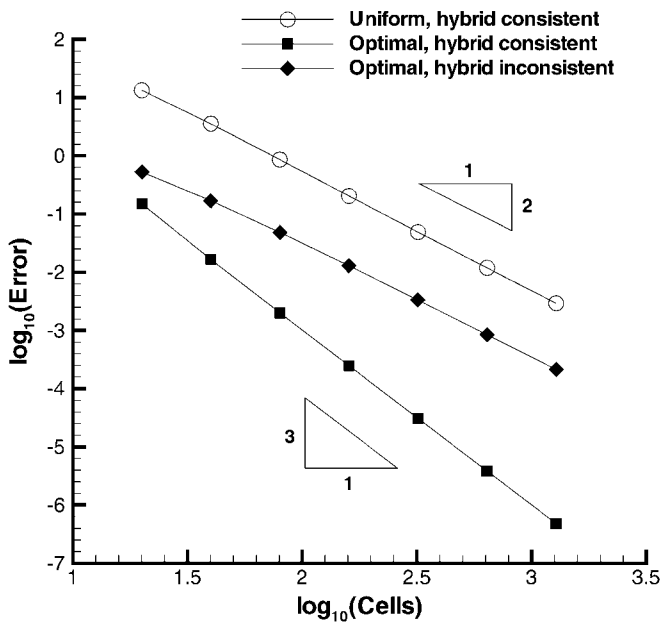

FIG. 17. Error convergence of a second-order hybrid approximation of f_x of Eq. (4.24), calculated with the consistent and inconsistent discretizations of the metric coefficient on the optimal and uniform grids.

with Eq. (4.24), regardless which second-order approximations are used for f_η, x_η, and y_η. However, if the metric coefficients x_ξ and y_ξ are evaluated by the two-point symmetric second-order difference expression in the entire computational domain, rather than at selected points as in the hybrid discretization, while both the hybrid approximation of f_ξ (4.3) and the optimal grid (4.24) remain the same, the result is that the order of the inconsistent approximation deteriorates to 2 and the truncation error increases by 10^3.

5. CONCLUSION

The new grid adaptation strategy based on the minimization of the leading truncation error term of an arbitrary pth-order finite difference discretization has been developed. The basic idea of the method is to redistribute grid points so that the leading truncation error terms resulting from the differential operator and the metric coefficients cancel each other. In that way, the design order of approximation on the optimal grid is increased by 1 in the entire computational domain. In contrast to most of the adaptive grid techniques, for the present method neither the truncation error estimate nor the specification of weighting parameters is required. Another very attractive characteristic of the new approach is its applicability to hybrid discretizations. It has been proven that if the differential operator and the metric coefficients are evaluated identically, then the same optimal grid adaptation criterion that is valid for nonhybrid discretizations can be used in the entire computational domain regardless of points where the hybrid difference operator switches from one approximation to another. One of the main advantages of the new method is that it can be directly extended to multiple dimensions. It has been shown that the multidimensional grid adaptation criteria are fully consistent with the one-dimensional counterpart. The 1-D and 2-D numerical calculations show that the truncation error obtained on the optimal grid is both superconvergent and reduced by several orders of magnitude in comparison with the uniform and standard adaptive grid results for all the test examples considered.

ACKNOWLEDGMENTS

The author thanks J. L. Thomas and M. H. Carpenter for many helpful discussions. This work was supported, in part, by the National Aeronautics and Space Administration under NASA Contract No. NAS1-97046 while the author was in residence at the Institute for Computer Applications in Science and Engineering and was performed, in part, while the author held a National Research Council Research Associateship Award at NASA Langley Research Center.

REFERENCES

1. J. F. Thompson and C. W. Mastin, Order of difference expressions on curvilinear coordinate systems, in *Proceedings of the ASME Fluid Engineering Conference on Advances in Grid Generation*, Houston, June 1983, p. 17.
2. J. D. Hoffman, Relationship between the truncation errors of centered finite-difference approximation on uniform and nonuniform meshes, *J. Comput. Phys.* **46**, 469 (1982).
3. E. Turkel, *Accuracy of Schemes with Nonuniform Meshes for Compressible Fluid Flows*, ICASE Report 85-43 (1985).
4. I. Babuška and W. Rheinboldt, A-posteriori error estimates for the finite element method, *Int. J. Numer. Meth. Eng.* **12**, 1597 (1978).

5. A. B. White, On selection of equidistributing meshes for two-point boundary-value problems, *SIAM J. Numer. Anal.* **16**(3), 472 (1979).
6. H. A. Dwyer, Grid adaptation for problems in fluid dynamics, *AIAA J.* **22**(12), 1705 (1984).
7. M. Letini and V. Pereyra, An adaptive finite difference solver for nonlinear two-point boundary problems with mild boundary layers, *SIAM J. Numer. Anal.* **14**(1), 91 (1977).
8. G. H. Klopfer and D. S. McRae, *The Nonlinear Modified Equation Approach to Analyzing Finite Difference Schemes*, Technical Paper 81-1029 (AIAA Press,Washington, DC, 1981).
9. V. E. Denny and R. B. Landis, A new method for solving two-point boundary-value problems using optimal node distribution, *J. Comput. Phys.* **9**, 120 (1972).
10. B. Pierson and P. Kutler, Optimal nodal point distribution for improved accuracy in computational fluid dynamics, *AIAA J.* **18**(1), 49 (1980).
11. D. Venditti and D. Darmofal, *A Multilevel Error Estimation and Grid Adaptive Strategy for Improving the Accuracy of Integral Outputs*, Technical Paper 99-3292 (AIAA Press, Washington, DC, 1999).
12. G. F. Carey and H. T. Dinh, Grading functions and mesh redistribution, *SIAM J. Numer. Anal.* **22**(5), 1028 (1985).
13. K. Chen, Error equidistribution and mesh adaptation, *SIAM J. Sci. Comput.* **15**(4), 798 (1994).
14. W. Rheinboldt, Adaptive mesh refinement processes for finite element solutions, *Int. J. Numer. Meth. Eng.* **17**, 649 (1981).
15. G. F. Carey and D. Humphrey, Mesh refinement and iterative solution methods for finite element computations, *Int. J. Numer. Meth. Eng.* **17**, 1717 (1981).
16. A. Mackenzie, D. F. Mayers, and A. J. Mayfield, Error estimates and mesh adaptation for a cell vertex finite volume scheme, *Notes Numer. Fluid Mech.* **44**, 291 (1993).
17. I. N. Bronshtein and K. A. Semendyayev, *Handbook of Mathematics* (Van Nostrand Reinhold, New York, 1985), p. 779.
18. J. U. Brackbill and J. S. Saltzman, Adaptive zoning for singular problems in two dimensions, *J. Comput. Phys.* **46**, 342 (1982).
19. J. F. Thompson, Z. U. A. Warsi, and C. W. Mastin, *Numerical Grid Generation: Foundation and Applications* (North Holland, New York/Amsterdam, 1985).